Electronic and Chemical Relations to Electrocatalytic Properties on $La_{0.7}Sr_{0.3}MnO_3$ Cathode Surfaces

Bilge Yildiz and Bulat Katsiev
Massachusetts Institute of Technology

Stefan Krause and Clemens Heske
University of Nevada – Las Vegas

Balasubramaniam Kavaipatti and Paul Salvador
Carnegie Mellon University

10th Annual SECA Workshop
July 15, 2009

Motivation: Surface electronic structure

Chemical reactivity should be sought for in the electronic structure of reactants.

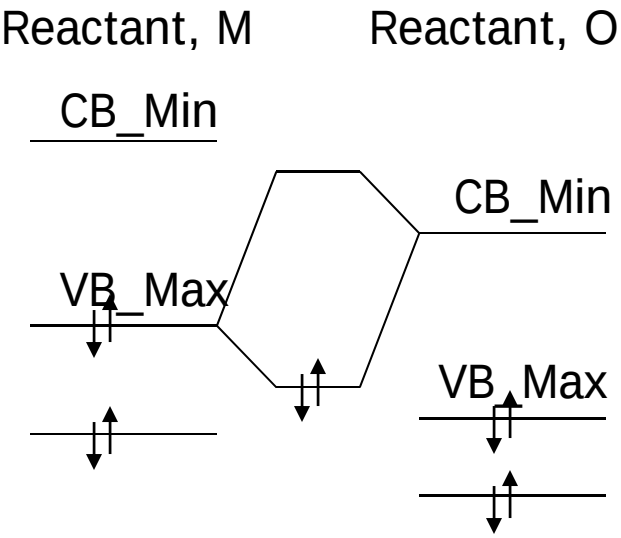

Energy levels of the electrons, which enter the interactions are important.

Inhomogeneities exist on the surfaces.

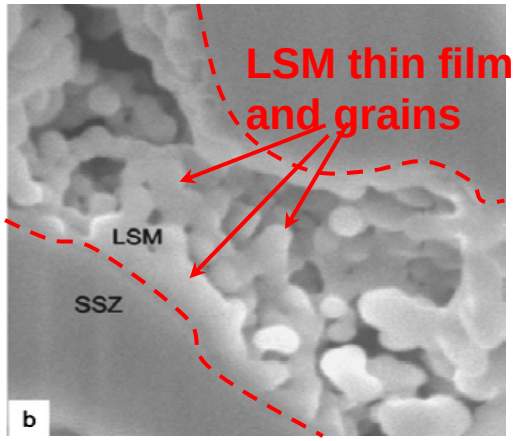

T. Sholklapper et al. *ESSL*, 10 (2007)

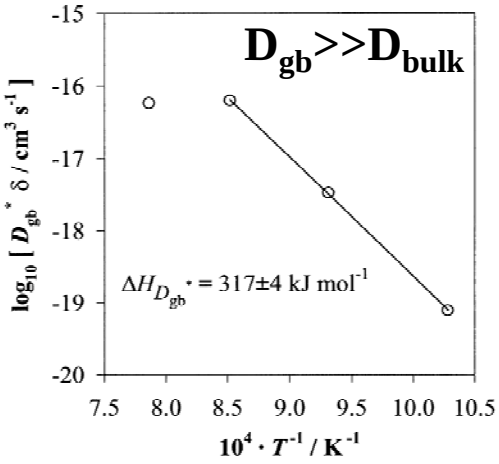

R.A. De Souza et al., *Mater. Lett.*, 43 (2000)

M. Petitjean et al., *J. Eur. Cer. Soc.*, 25 (2005)

Inhomogeneities can favor fast charge transport.

Objective and approach

Surface topography and electronic structure in bond breaking and formation: Scanning Tunneling Microscopy/Spectroscopy (STM/STS)

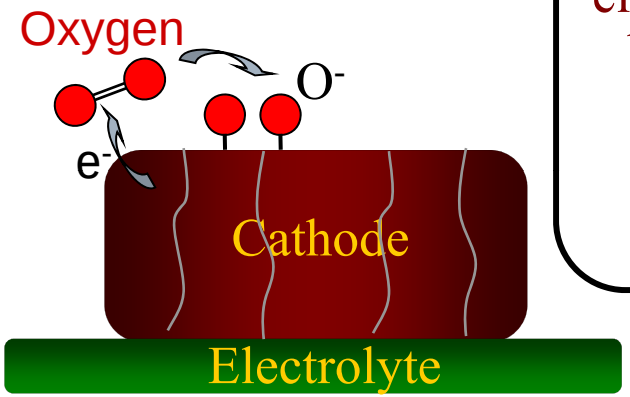

Surface chemical and electronic structure in bond breaking and formation, laterally averaged; UV/Soft X-ray spectroscopies

Understand the electronic and chemical behavior on SOFC cathode surfaces for electrocatalysis of oxygen, in the presence of inhomogenities.

Model dense thin-film cathode structures

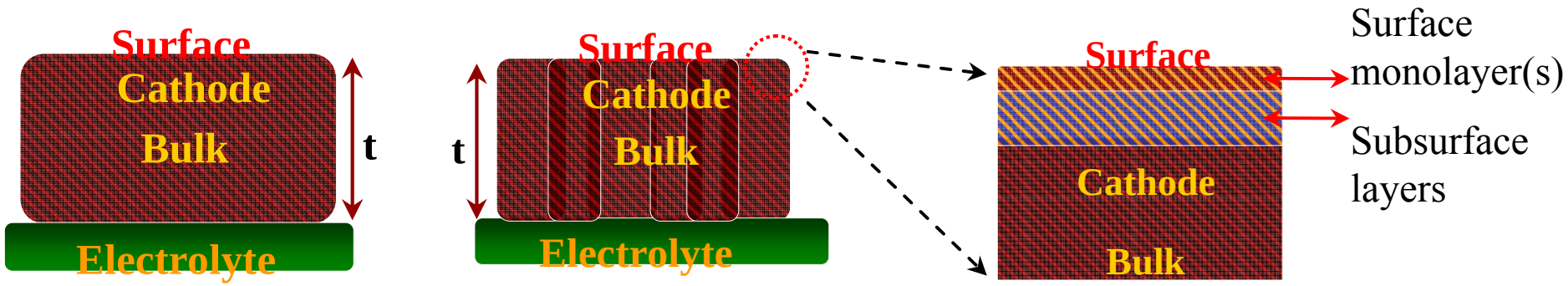

A- Epitaxial:

1. Stable crystallographic orientations.
2. Strain, due to lattice mismatch, or thickness variation

B- Textured polycrystalline:

1. Stable crystallographic orientations.
2. Grain boundary structure, composition, and charge.

Stable termination layers on the cathode film. E.g., LaO vs. MnO termination on LSM surface.

Scanning Tunneling Microscopy (STM)
Scanning Tunneling Spectroscopy (STS)

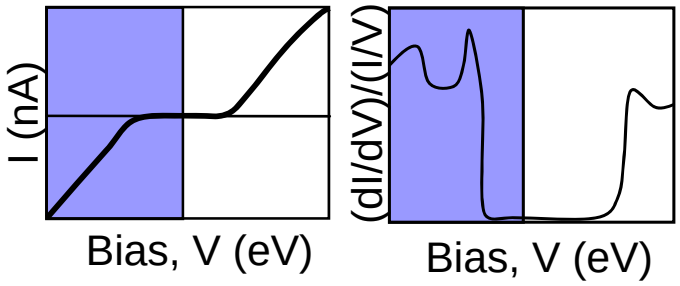

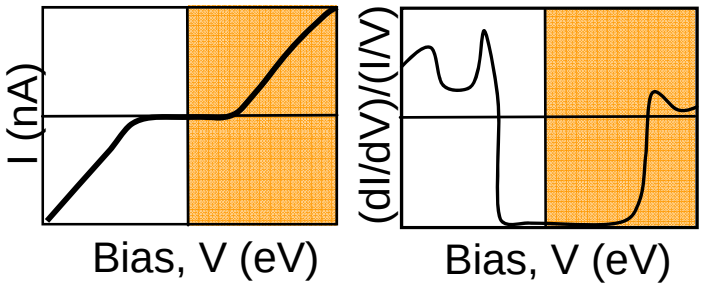

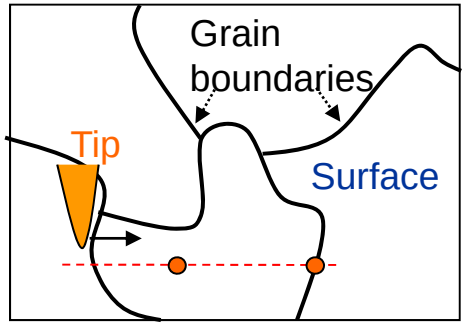

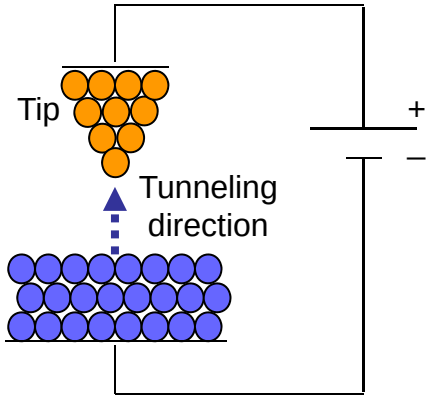

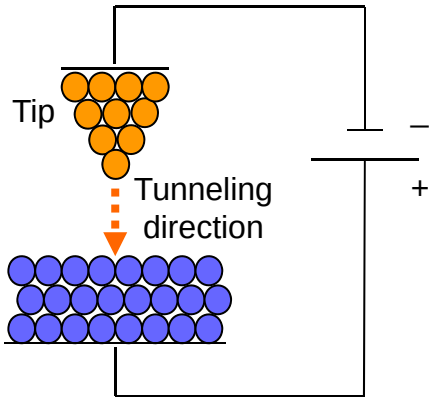

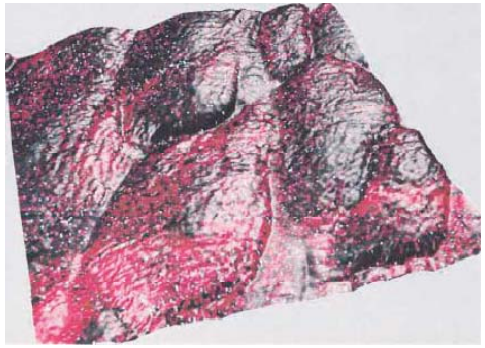

Fermi-level tunneling conductance map on $La_{0.8}Ca_{0.2}MnO_3$.

T. Becker, C. Streng, Y. Luo, et al., *Phys. Rev. Lett.* 89 (2002).

- Probing the filled (valance band) electronic states.
- Probing the empty (conduction band) electronic states.

UV/Soft X-ray Spectroscopies

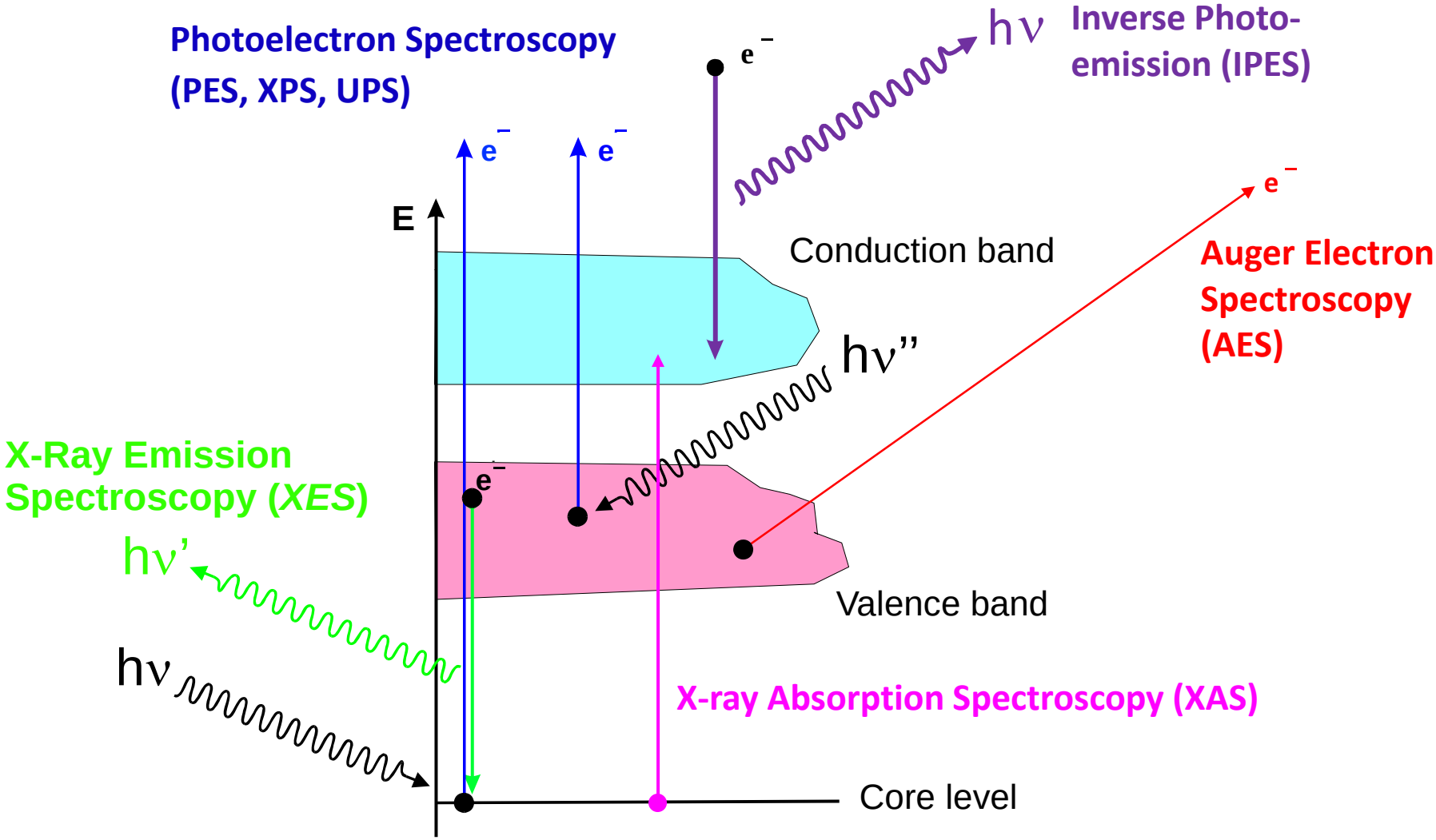

STM/STS set-up and experiment conditions

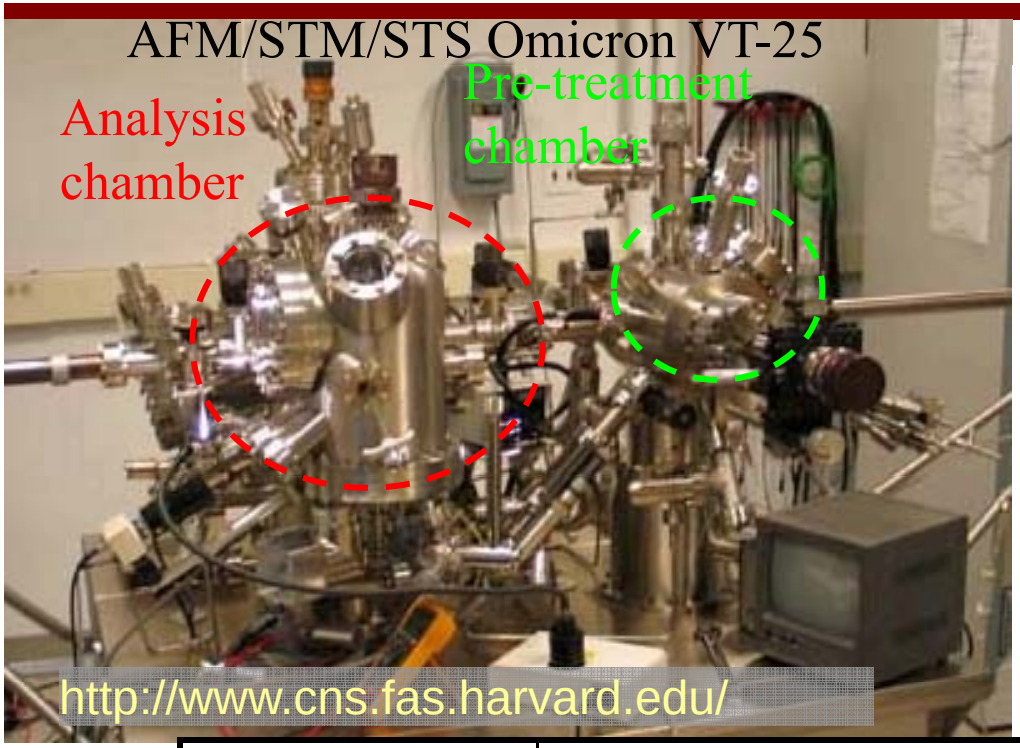

Analysis chamber:
High temperature (upto 1100K)

Pre-treatment chamber:
High temperature (upto 1100K)
Electrochemical control possibility

	Ex situ	***In situ***
Pre-treatment Conditions	T = 500 – 700°C $P_{O2} = 10^{-8} – 10^{-7}$ mbar t = 1 hr	
Measurement Conditions	T = 23°C $P_{O2\text{-base}} = 10^{-10}$ mbar	T = 300 – 580 °C $P_{O2\text{-base}} = 10^{-6}$ mbar, dosing surface from 2 bar, $P_{O2\text{-surface}} = 10^{-4} - 10^{-3}$ mbar

$La_{1-x}Sr_xMnO_{3+d}$ defect chemistry at a range of P_{O2}

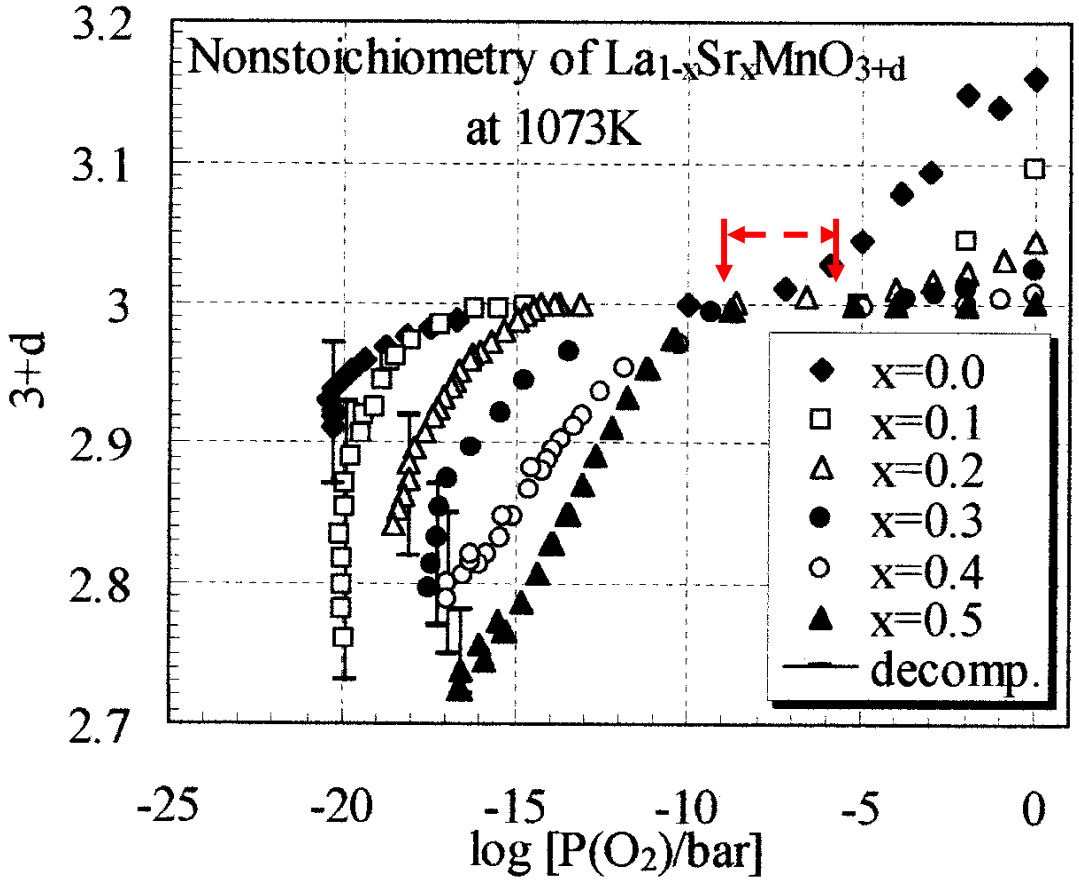

Nonstoichiometry, $La_{1-x}Sr_xMnO_{3+d}$ (x=0-0.5) as a function of P_{O2}.

J. Misuzaki et al. *SSI*, **132**, 2000, pp.167

LSM bulk should not reduce in our experiment conditions thus far.

Questions to highlight

- What is the effect of thickness of dense thin-film cathodes on surface topography, composition and electron tunneling?

- Where do the inhomogenities in surface electronic structure arise from?

- How do the surfaces evolve in electronic and chemical state with temperature in oxygen environment?

All our experiments reported here, on $La_{0.7}Sr_{0.3}MnO_3$, Pulsed Laser Deposited on YSZ(111) single crystal substrates.

LSM surface topography by STM

10nm-thick, Z_{range}= 4nm

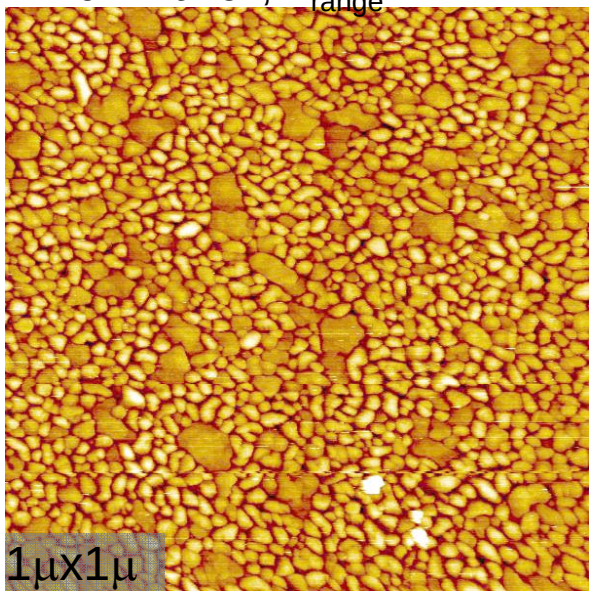

50nm-thick, Z_{range}= 6nm

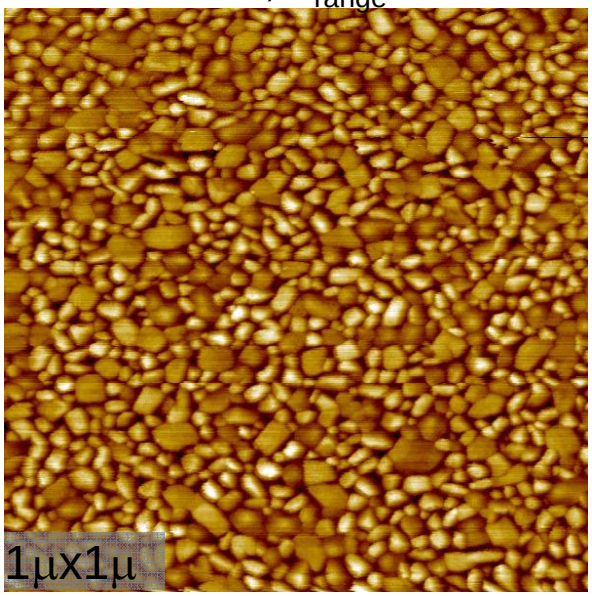

100nm-thick, Z_{range}= 9nm

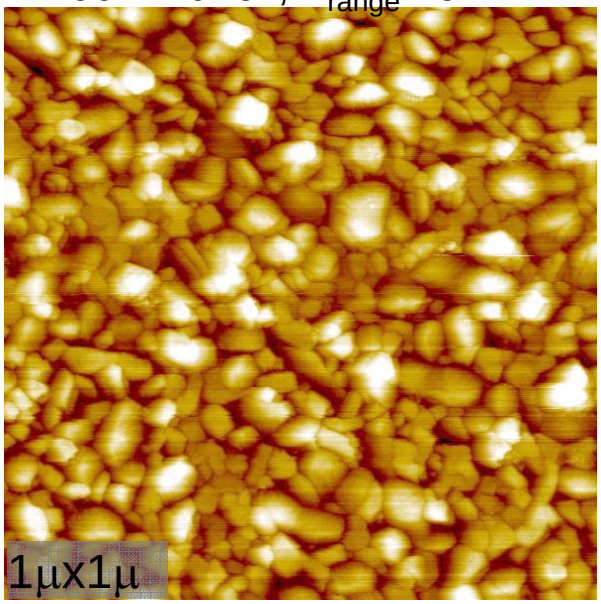

Images at RT, 10^{-10} mbar

- Two types of grains coexisted, without an apparent orientation in the topographic images:
  - Large island-type flat grains, 70-140nm,
  - Smaller grains, 30-50nm.

10nm-thick LSM surface topography

RT, $P_{O2\text{-}surface} = 10^{-10}$mbar

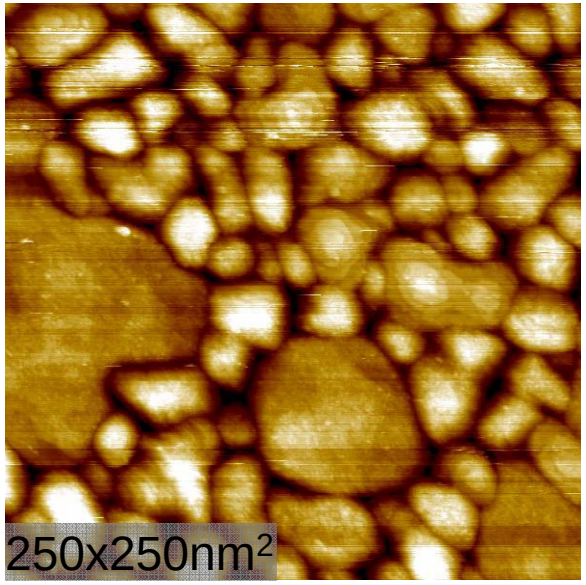

580°C, $P_{O2\text{-}surface} = 10^{-4}$-$10^{-3}$ mbar

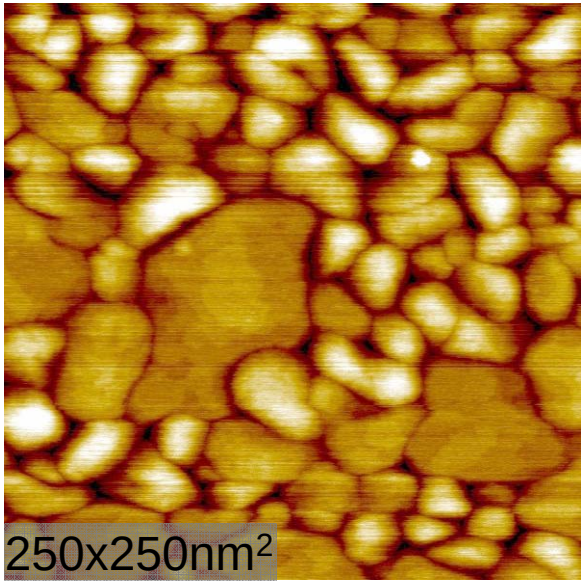

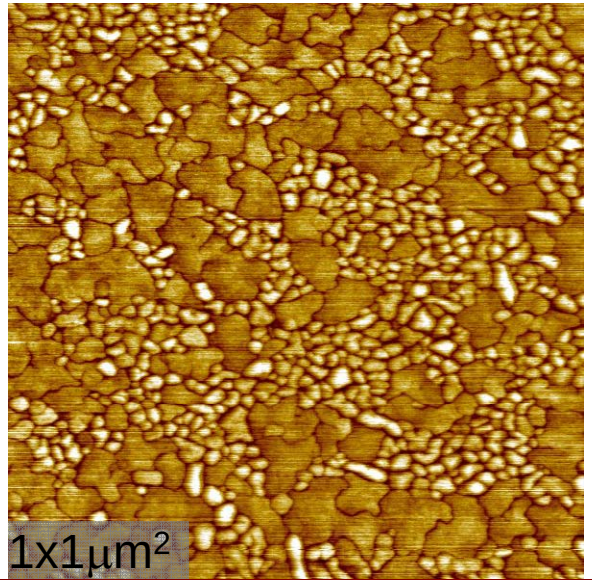

- Step-edges resolved both at RT and at 580°C in oxygen.

Fraction and size of large islands (grains) grow with time (for ~24 hrs) at high temperature, probed *in situ*.

LSM surface composition by AES

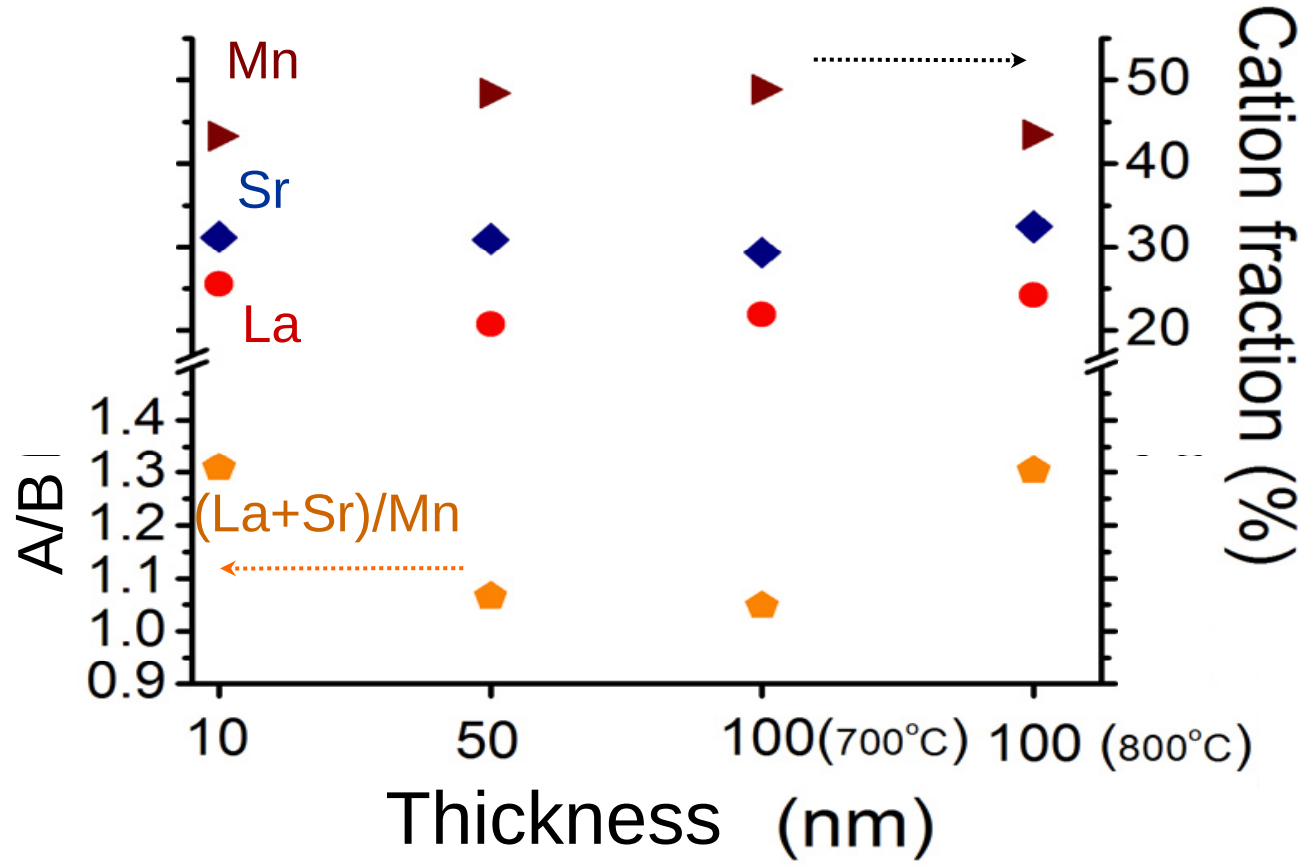

- Surfaces enriched in A-site, 1.05 < A/B < 1.3.
- Surface composition depends on thickness and deposition temperature.
  - Thickness ↑, A/B ↓.
  - $T_{deposition}$ ↑, A/B ↑.

LSM surface chemistry by XPS

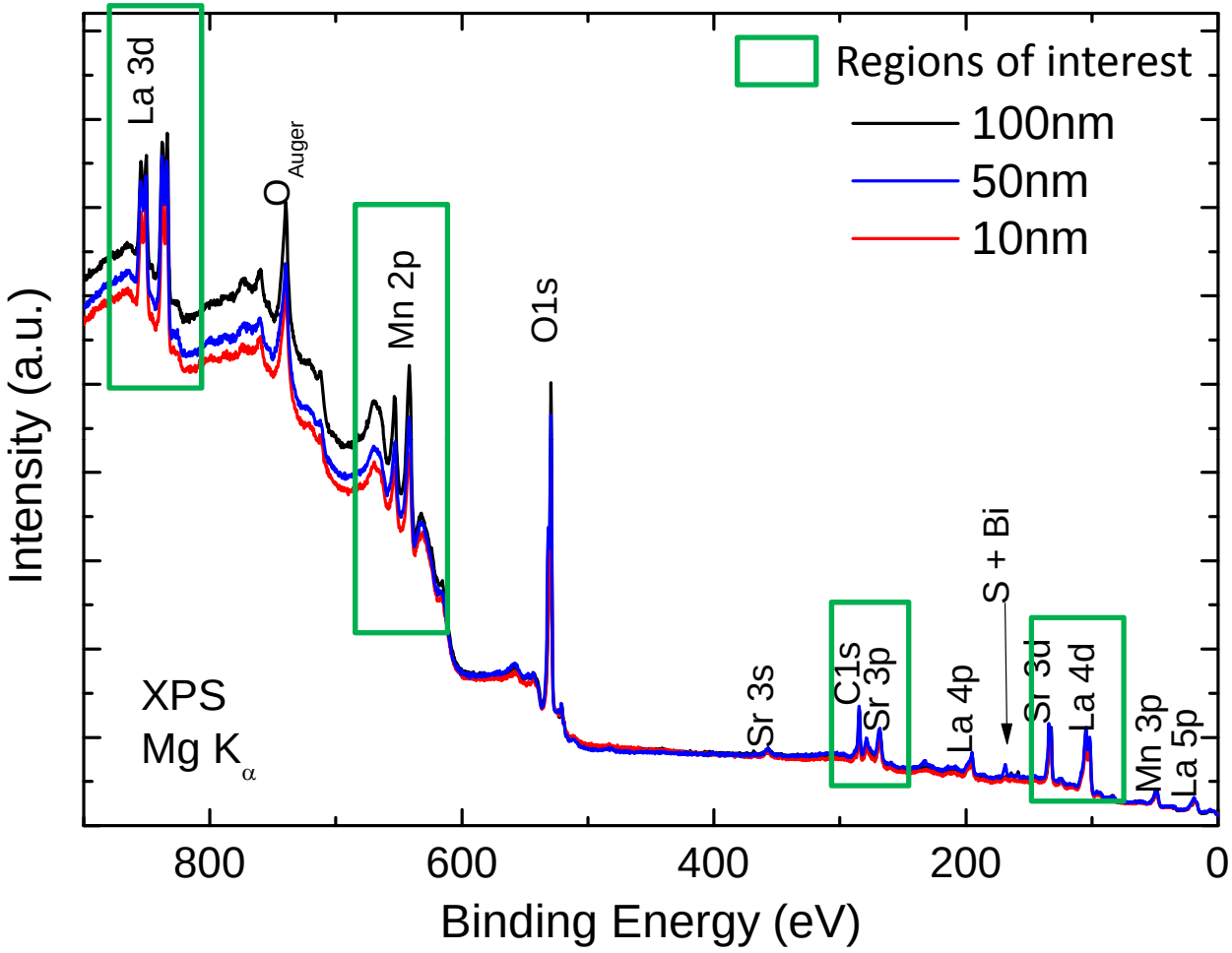

- XPS: very accurate to determine *relative* changes of a line;
  - ratios of elements (lines) that are close in energy (only require photoionization cross sections)

LSM surface composition by XPS

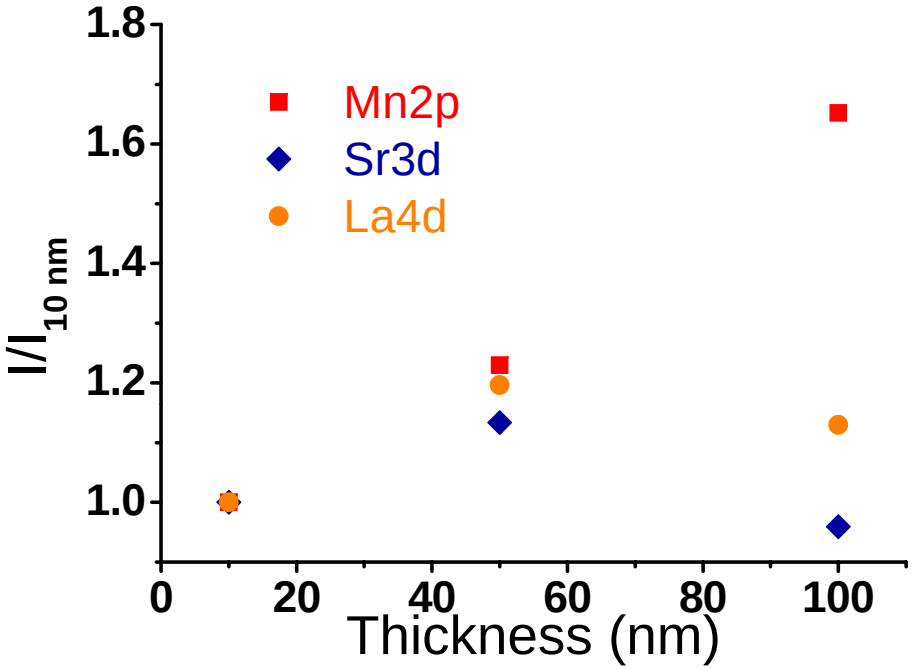

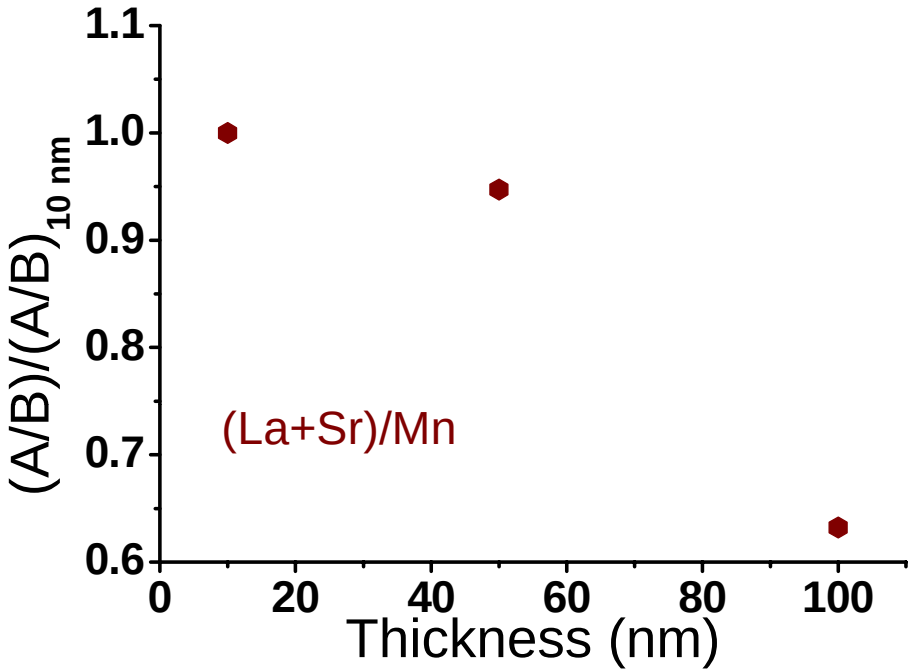

- Sr and La show only small variations with thickness
- Mn signal increases with increasing film thickness
- A/B ratio decreases with increasing thickness

Variation in the electronic behavior probed by STS

50nm-thick LSM surface

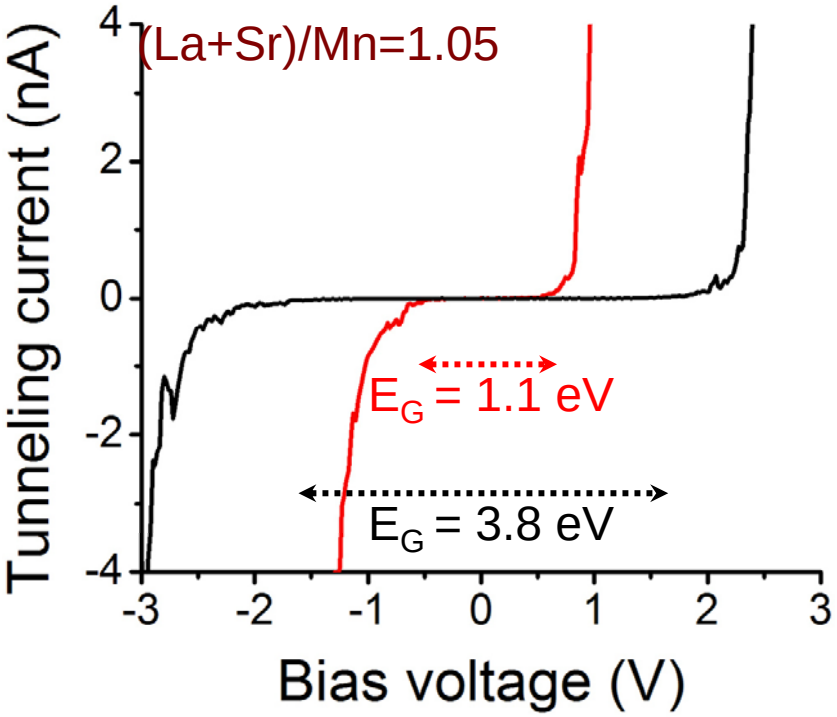

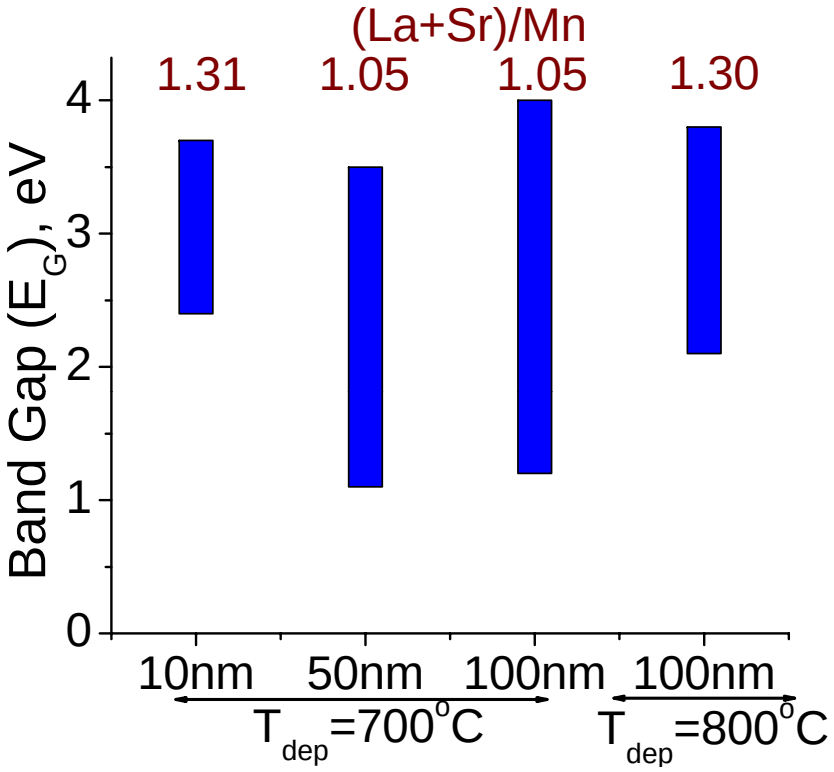

- "Smaller thickness" and "higher $T_{deposition}$" lead to:
  - larger A/B ←→ large E_G, more insulating in STS.

Surface-limited ORR on "thinner" LSM

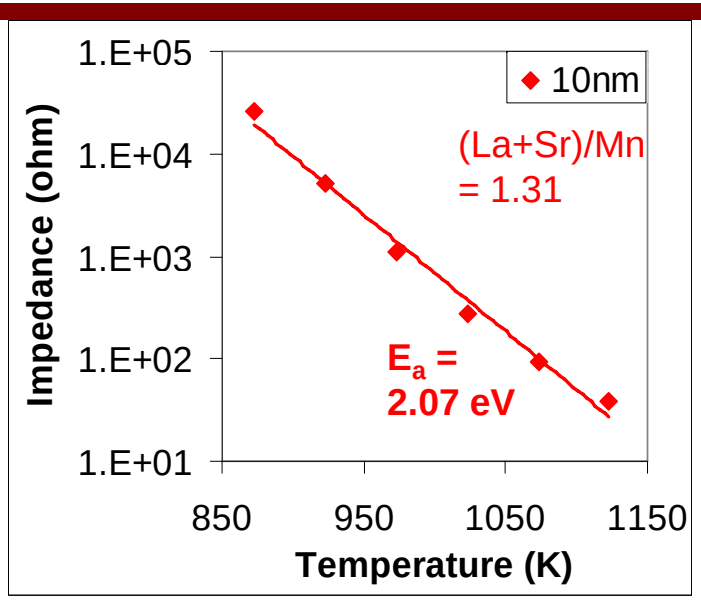

2.07 eV → surface-limited 600-850°C.

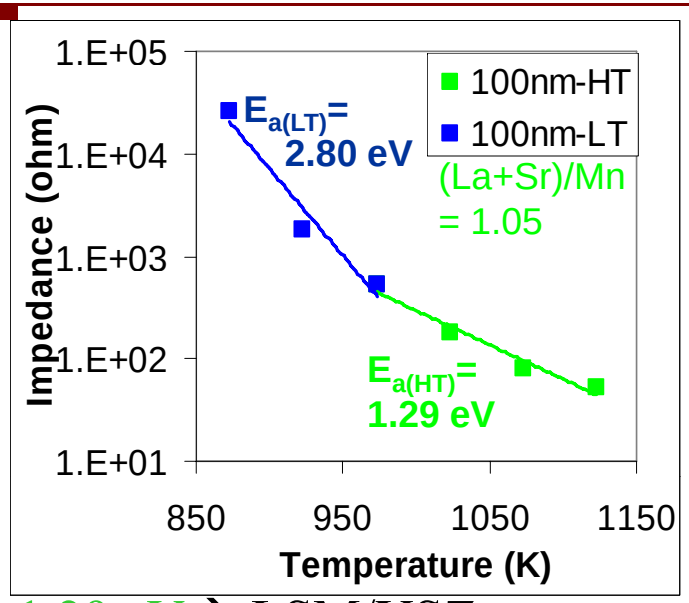

1.29 eV → LSM/YSZ interface at 700-850°C.

2.80 eV → $O^{=}$ diffusion in the bulk of LSM at 600-700°C.

A less enriched A-site chemistry lead to more favorable surface for ORR electrochemistry on thicker LSM films on YSZ.

J. Van Herle et al., *Electrochim. Acta*, 41 (1996)
M. J. Jorgensen et al., *J. Electrochem. Soc.* 148 (2001)
Y. Arachi et al., *Solid State Ionics*, 121 (1999)
G.J. la O' et al., *J. Electrochem. Soc.*, 154(4) (2007)

Key observations and hypothesis

- What is the effect of thickness of dense thin-film $La_{0.7}Sr_{0.3}MnO_3$ (LSM) cathodes on surface, composition, and electronic structure?
  - Thinner LSM surfaces →
    - have A-site rich surfaces in AES,
    - are more resistive (large E_G) in STS (RT),
    - show surface limited ORR in EIS.

Recall: Inhomogenities in surface electronic structure

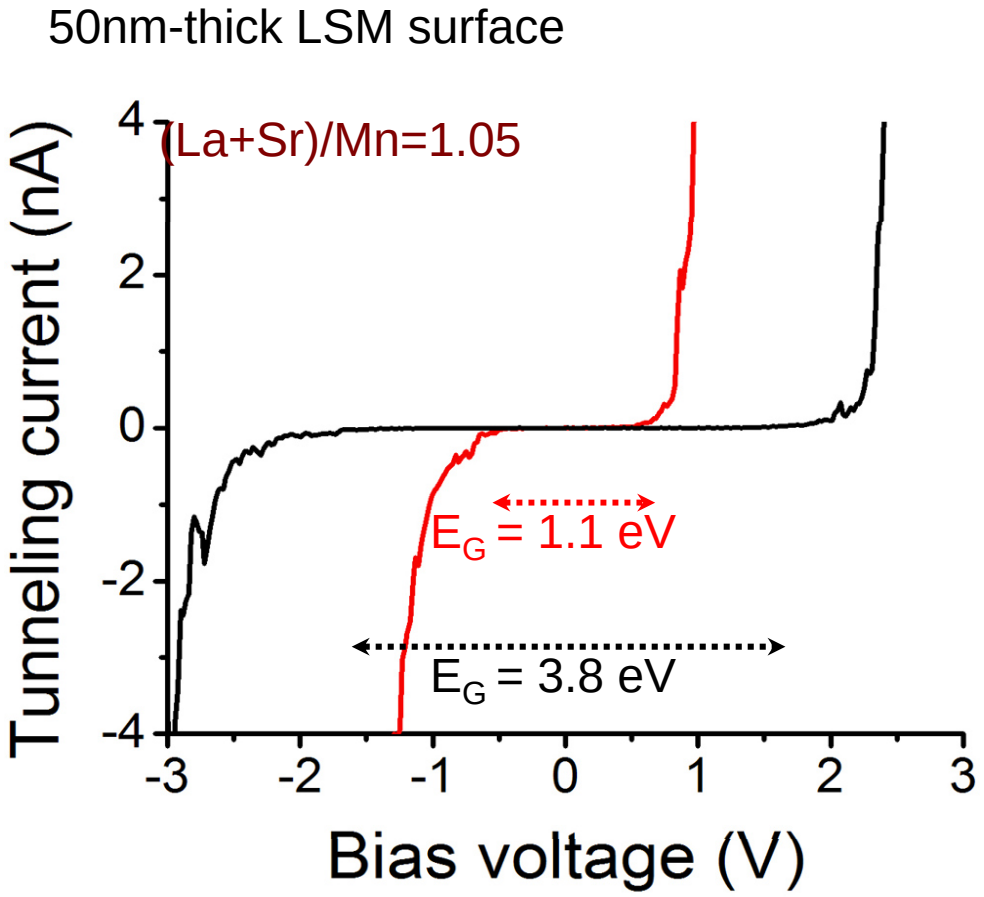

- Pristine versus complicated surfaces?

Variation of STS Spectra: possible reasons
1) Multiple phases on the surface

Ab initio thermodynamics predictions:

- Sr makes the (La,Sr)O-terminated surfaces stable at RT, along with MnO_2-terminated surfaces
- At 800°C, (La,Sr)O-termination favorable.

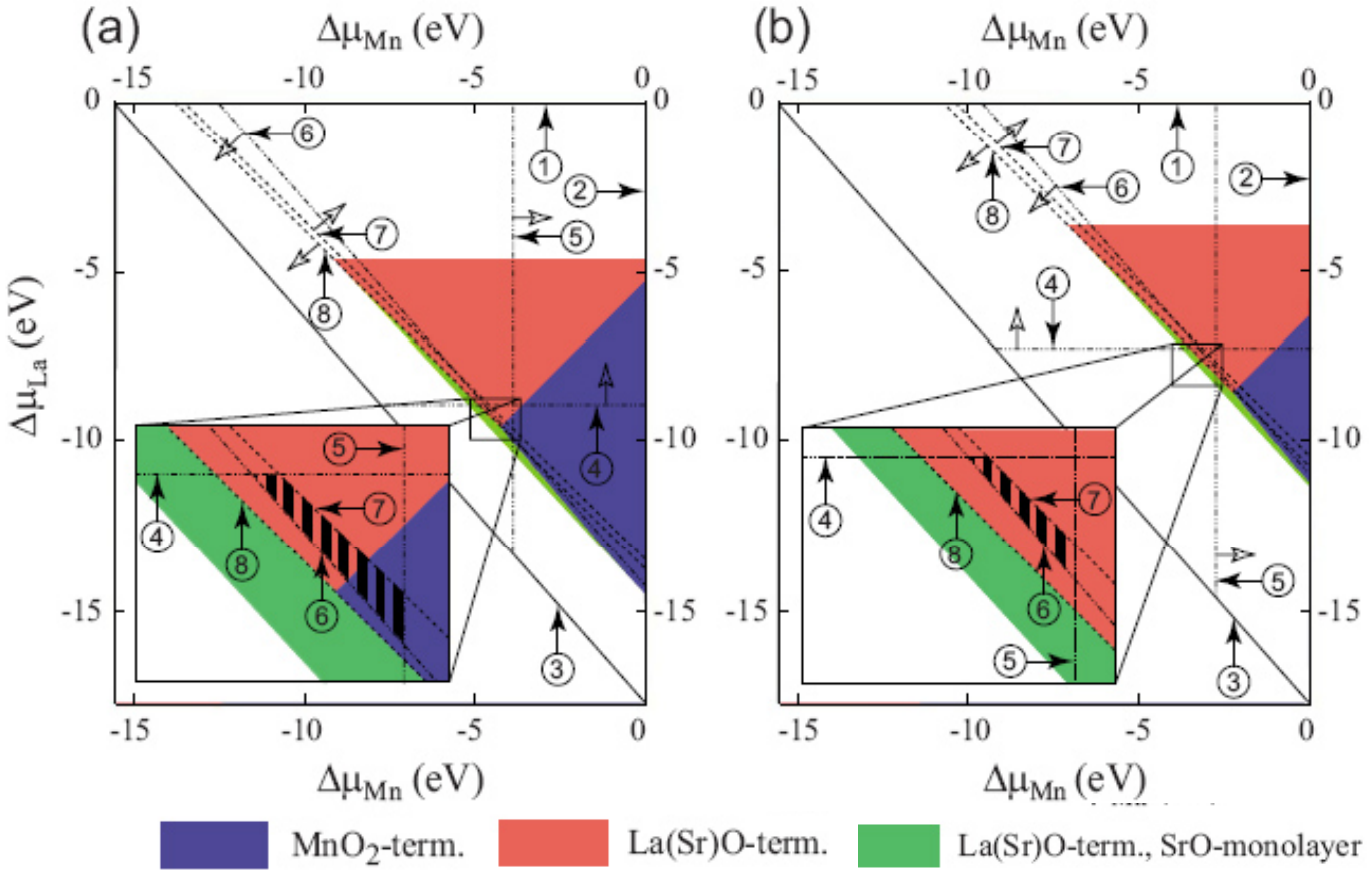

Band gaps:

$SrMnO_3$: 1.2eV
$LaMnO_3$: 1.7eV
MnO_2: 2.8eV
La_2O_3: 4.3eV
SrO: 5.5eV

Piskunov et al, Physical Review B 78, (2008) 121406R

Variation of STS Spectra: possible reasons
2) Various defect configurations on the surface

Unoccupied states image, at 1.5V

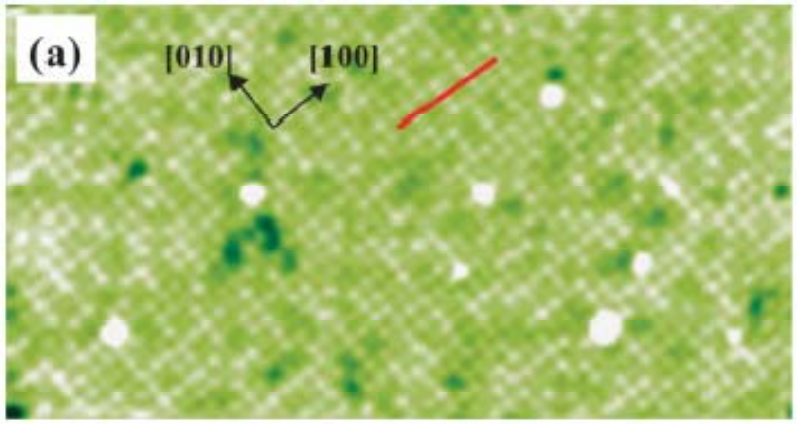

Occupied states image, at -2.0V

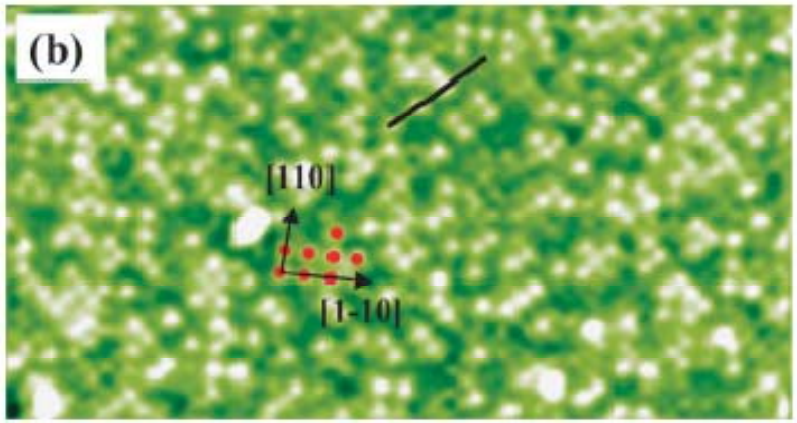

J. X. Ma et al., *Phys. Rev. Lett.*, 95 237210 (2005)

Surface defects of the $(La_{5/8-0.3}Pr_{0.3})Ca_{3/8}MnO_3$ (paramagnetic) surface were reported to form short-range nanoscale charge-order-like clusters with varying electronic tunneling characteristics.

Key observations and hypothesis

- Where do the inhomogenities in surface electronic structure arise from?
  - Presence of multiple oxide phases?
  - Presence of multiple defect configurations?

Where else are the inhomogenities along with topography?

Tunneling current, I_{tunnel}, correlated with boundaries and/or domains?

Topography map

150x150nm^2

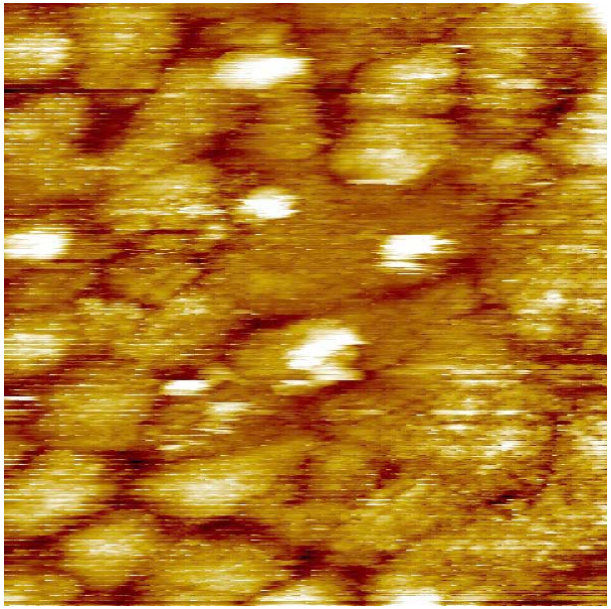

I_{tunnel} map, at -2.2V

- Higher electron tunneling rate at select grain boundaries compared to grain surfaces.

I_{tunnel} correlated with grain boundaries: Chemical or structural reasons?

- Dopant segregation or structural disorder at the GB, leading to a space charge region with charged defect concentration variation?

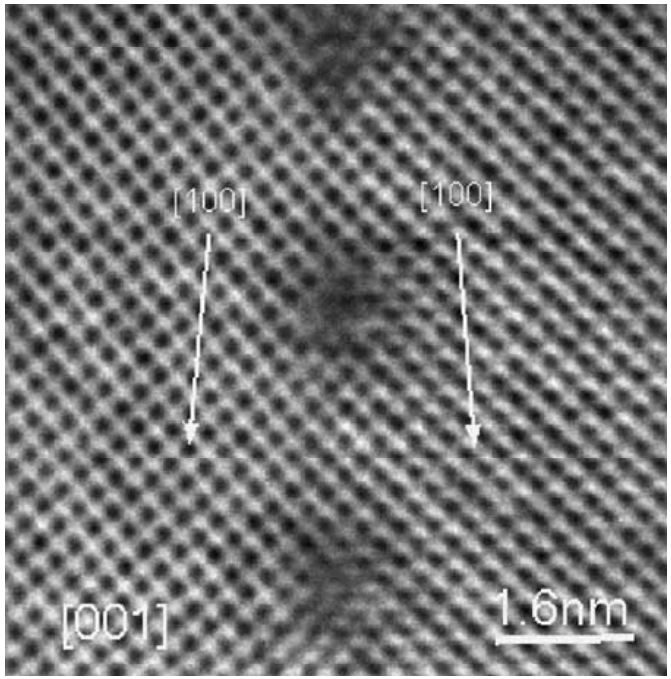

Dislocation cores at low angle tilt GB in $SrTiO_3$:

→ Positive charge at GB due to oxygen depletion, surrounded by space charge.

Zhang and De Souza et al. *Acta Mater*. **53** (2005)

I_{tunnel} correlated with boundaries and/or domains: Chemical or structural reasons?

- LSM : Higher tunneling near the GB could result from a charged core and surrounding space charge with hole concentration near the GB.
  - Thermodynamically driven oxygen vacancy at the GB, lead to Mn^{3+} at the core, and holes (Mn^{4+}) in the space charge region.

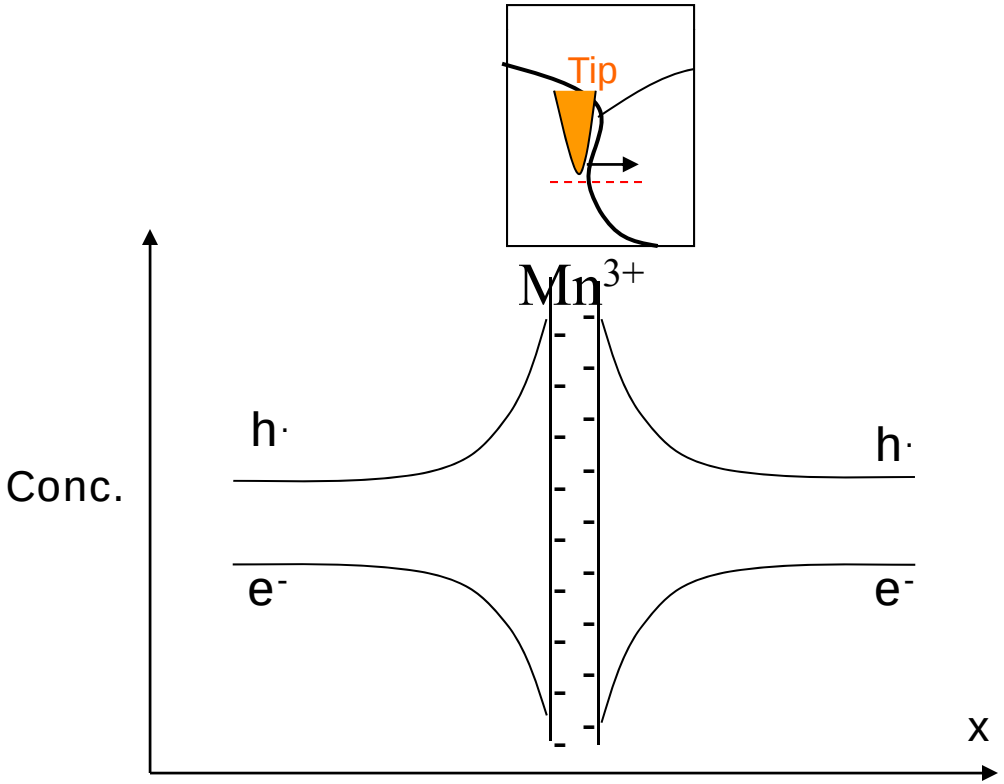

High temperature – ex situ - chemistry by XPS

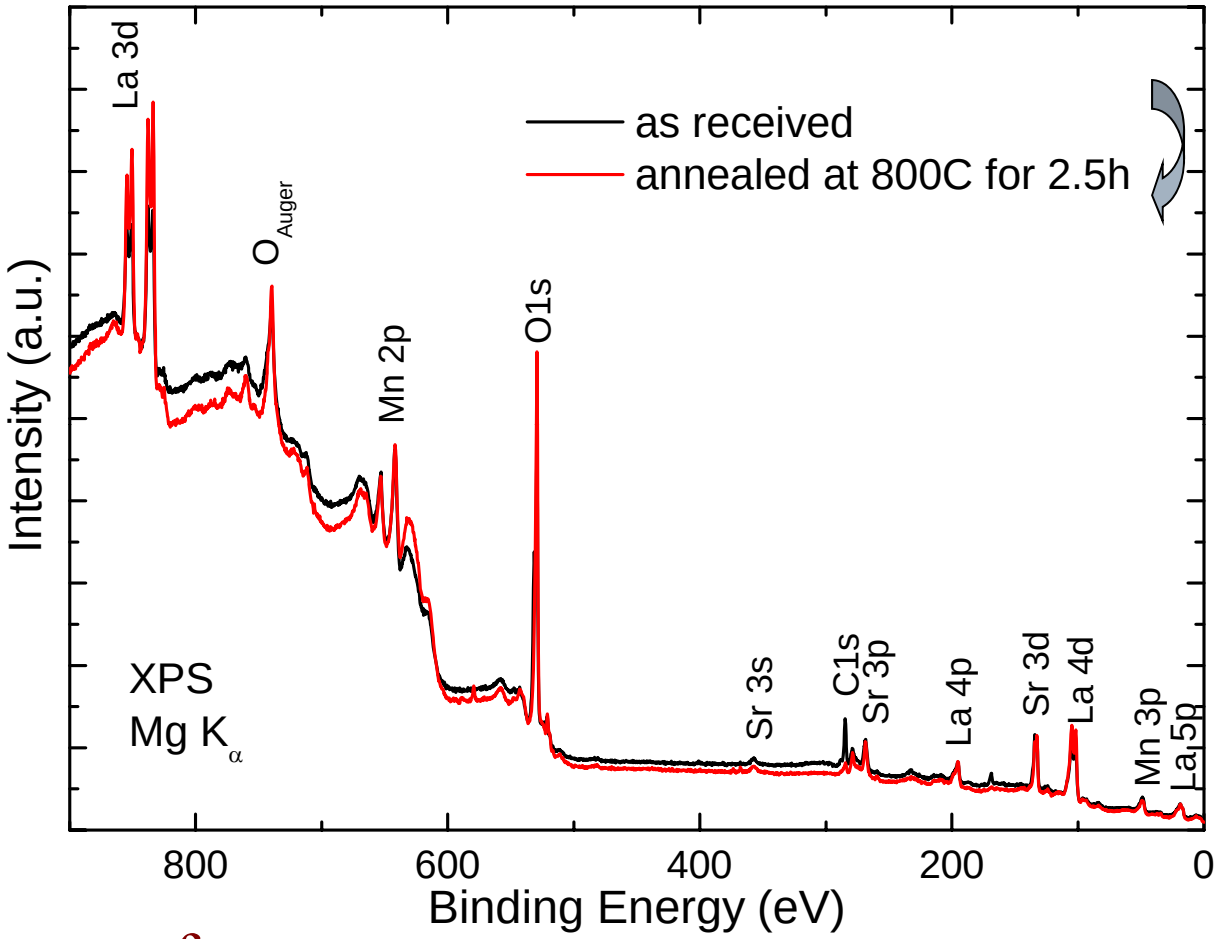

A/B= ↑
(La+Sr)/Mn

- Increase of oxygen content
- Mn and Sr signals show no relative changes
- La increases by 100%, surface-sensitive (using La 3d, more)
  by 20%, more bulk-sensitive (using La 4d)

High temperature – in situ - chemistry by AES

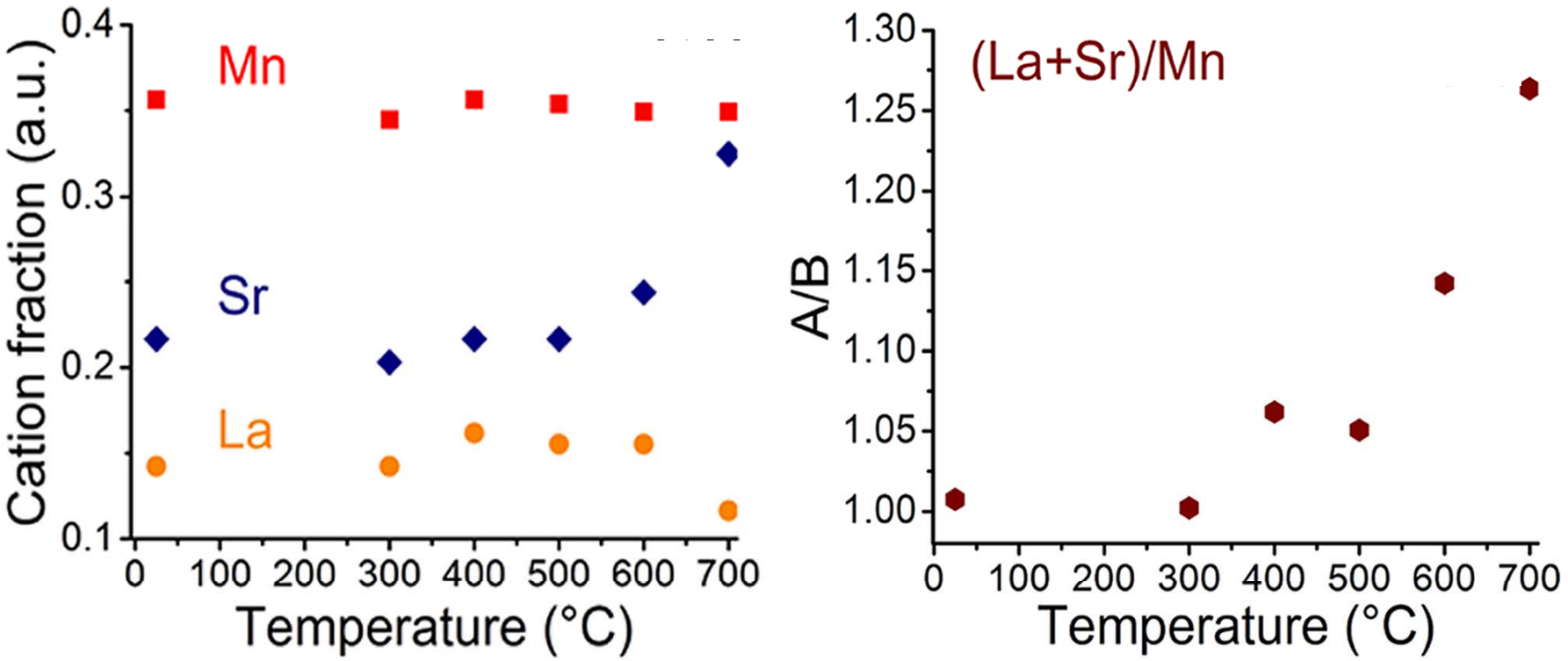

Surface A- and B-site cation fractions at P_{O2}= 10^{-6} mbar.

- (La+Sr)/Mn:
  - does not change up to 500°C, and
  - increases above 500°C.

Katsiev and Yildiz et al., *APL*, accepted 07/09

High temperature electronic behavior probed by STS

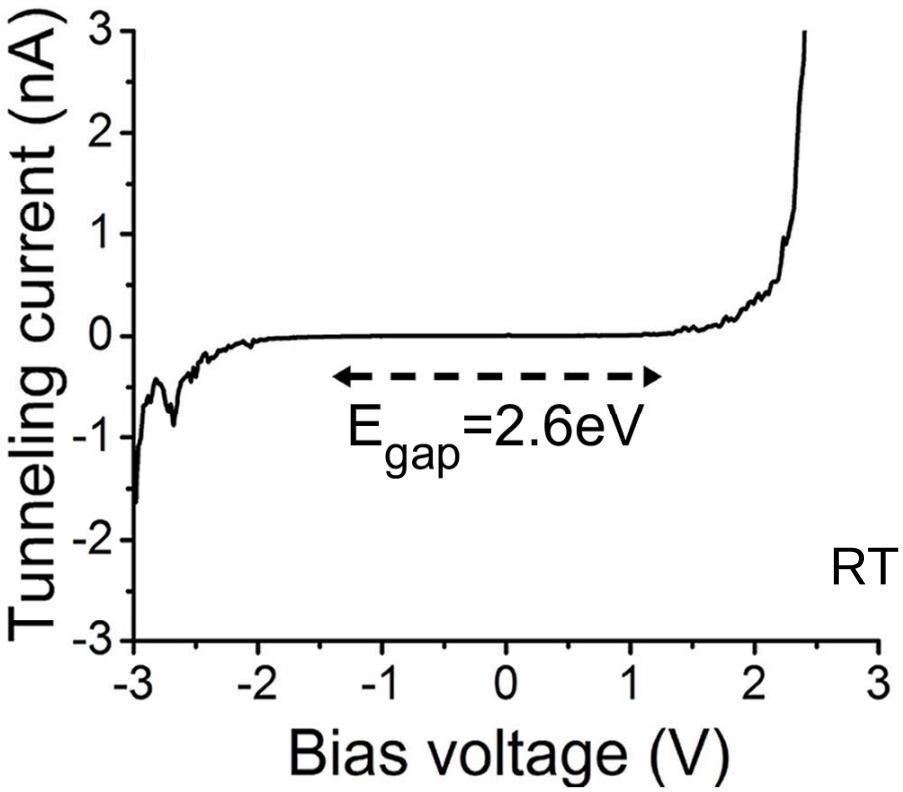

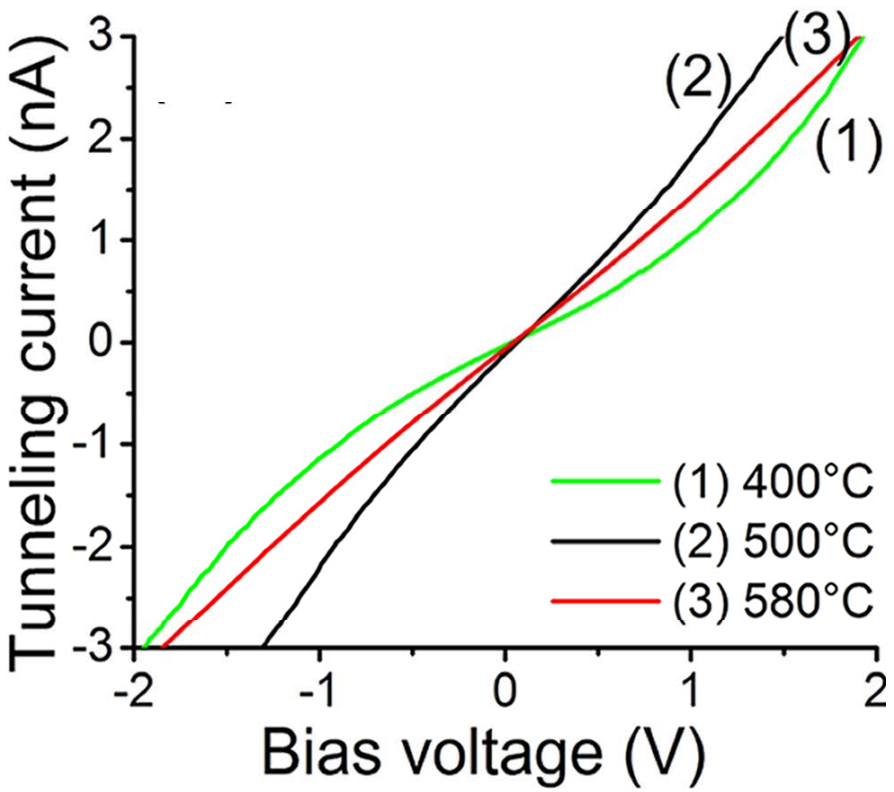

- Tunneling conductance:
  - increases with temperature from RT to 500°C, and
  - decreases above 500°C to 580°C .

Katsiev and Yildiz et al., *APL*, accepted 07/09

High temperature electronic behavior: possible reason

- Band gap → metallic transition?:

1) Reduction of the oxide to metal?
   → AES shows strong oxygen peak, to the contrary.

2) Further oxidation of the surface of a p-type conductor?
   Mn-O → Mn^{4+} with $h^{\cdot}$

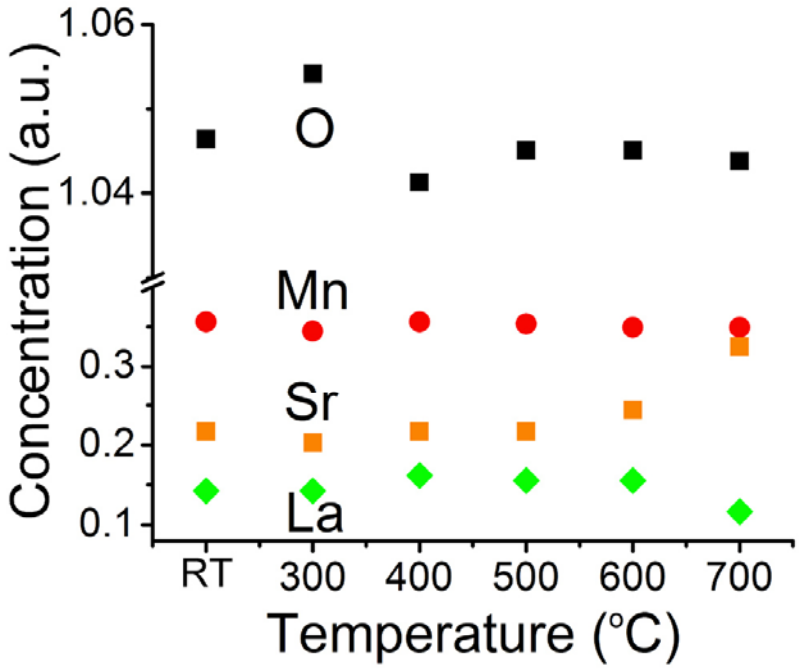

3) Structural transformation at the surface? e.g. like that from an orthorhombic phase (characterized by a strong Jahn–Teller distortion) as an insulating state, to a rhombohedral phase with a metallic state.

High temperature electronic behavior: possible reason

■ Tunneling conductance decrease 500 → 580°C?: Thermodynamically driven evolution of a Sr-rich phase accompanied by the relative decrease of Mn on the surface.

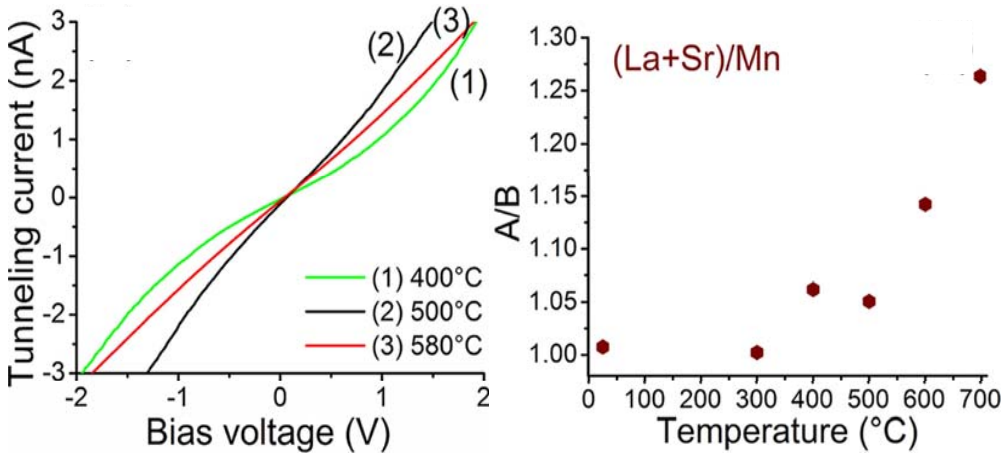

■ Suggests that the A-site and/or Mn-poor surfaces are less active for electron exchange in oxygen reduction on LSM.

"Strong oxygen binding and high O-vacancy formation energies suggest LaO-terminated surfaces are catalytically inactive."

Y-L. Lee, D. Morgan, et al.,
214th Meeting Electrochemical Society, Honolulu, HI, 2008

Key observations and hypothesis

- How are the surfaces evolving in electronic and chemical state with temperature in oxygen environment?
  - I_{tunnel} ↑ upto 500°C, followed by a ↓
  - A-site ↑ above 500°C

Hypothesis: Re-structuring or oxidation state-change at lower temperature, and Sr-driven chemical changes at high temperature?

Summary remarks

Common theme: Decrease in (La+Sr)/Mn →
increase in surface tunneling at RT and HT,
increase in surface activity in ORR

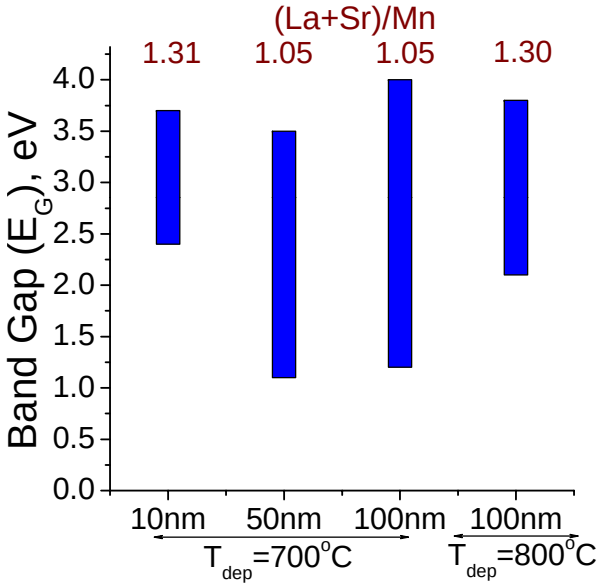

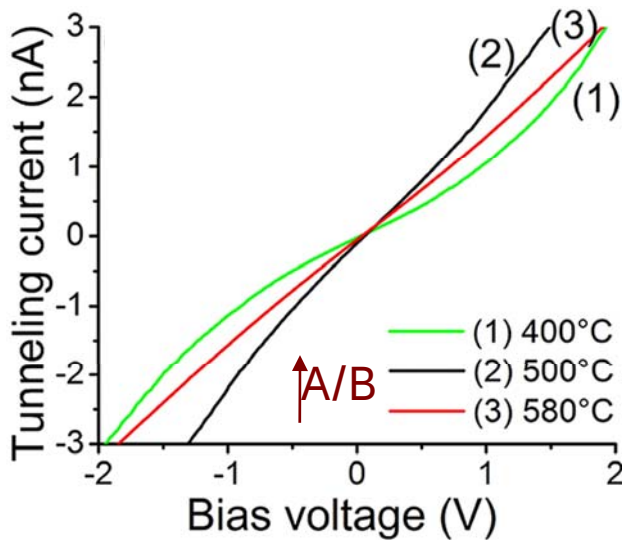

In agreement with electrochemical activation of LSM and LSCF surfaces.

G.J. la O', PhD Thesis, MIT, 02/2008.

Baumann et al. *JECS*, **152**, 2005.

Co-existence of multiple oxides, role of defect configurations and space charge regions seem evident, and need to be probed more in depth, and *as-in situ-as* possible.

Future work

- Identify the origin and nature of:
  - electronic inhomogenities due to multiple oxides and/or defects, using epitaxial well-defined LSM surfaces,
  - transition from large-E_G to metallic above room temperature.

- Valence band and core level information from the XES and XAS data taken at the Advanced Light Source (ALS) (currently being processed).

- In-situ x-ray emission/absorption at the ALS.

- Extend studies to LSCF.

Acknowledgements

- Research in part conducted at the Center for Nanoscale Materials of NSF at Harvard University.
- Constructive discussions with Dr. Hoydoo You (ANL), and Dr. Briggs White and Mr. Wayne Surdoval.
- Financial support by DOE-FE Solid State Energy Conversion Alliance, and Argonne National Laboratory.

33

Sharp drop in I_{tunnel} at positive bias, $+V_{th}$

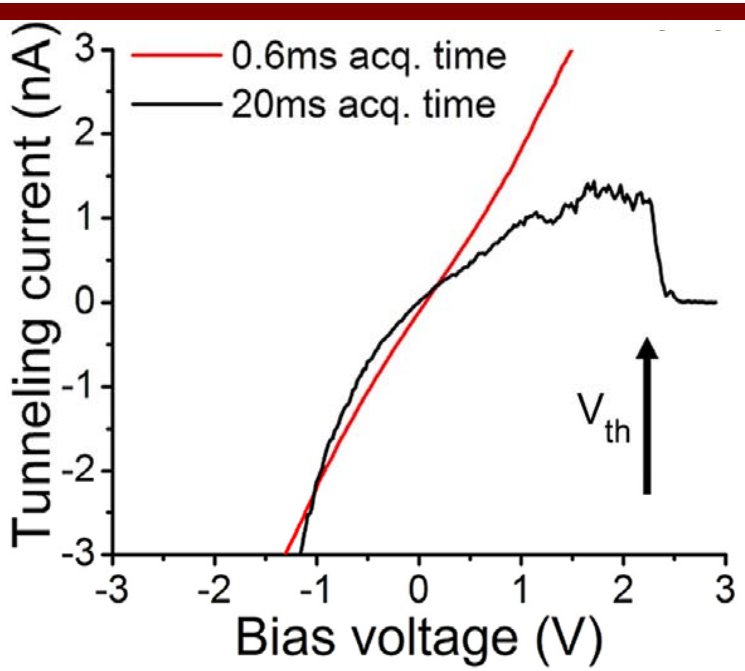

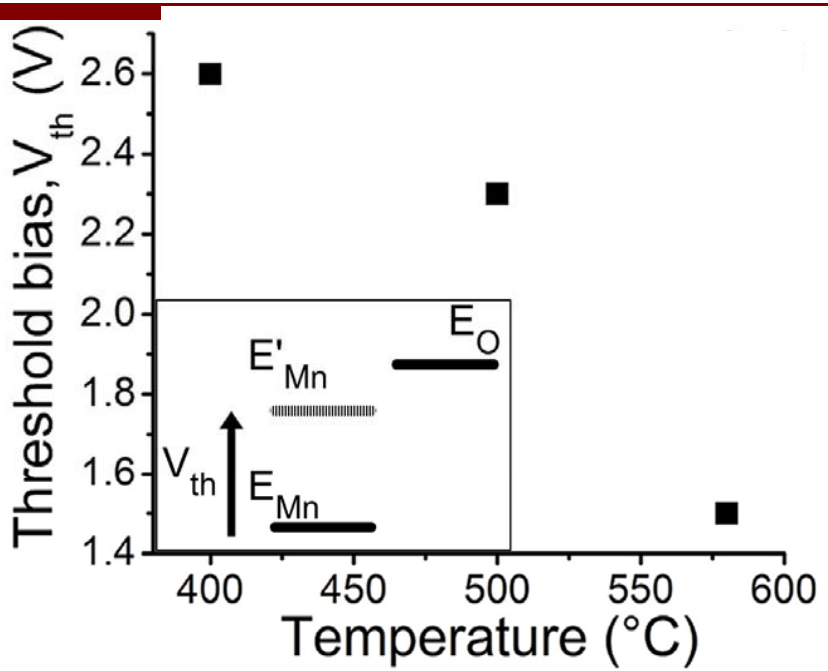

- T-, t-, and V-dependent drop in I_{tunnel} → chemical reaction, (possibly) oxygen binding on LSM surface.
- $V_{th,}$ at a given temperature, could be used as probe of activation polarization for surface-oxygen bonding.

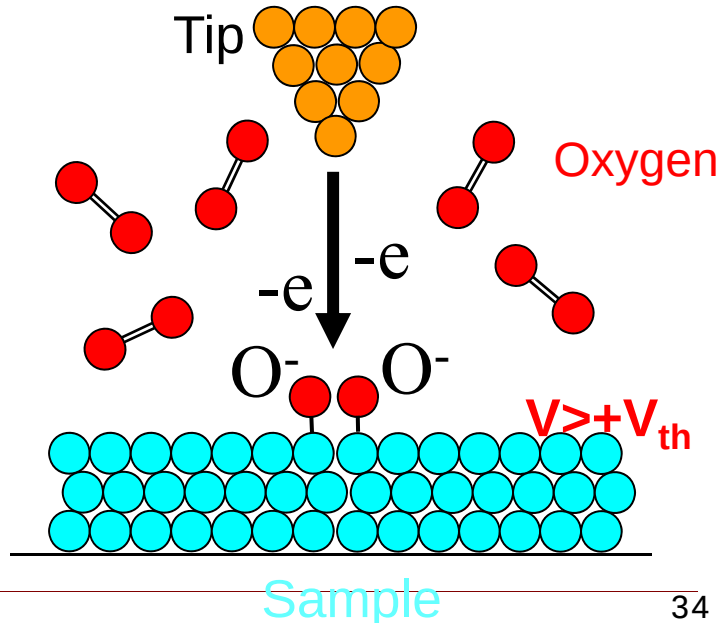

Bias-induced oxidation

- Bias-induced localized (nanometric) oxidation accompanied by the drop in tunneling conductance is reported on Si and GaAs surfaces at room temperature.
- Binding of oxygen from the gas phase on the dangling bonds of the surface, results in the formation of the atomically localized or nanometric dimension oxide area.

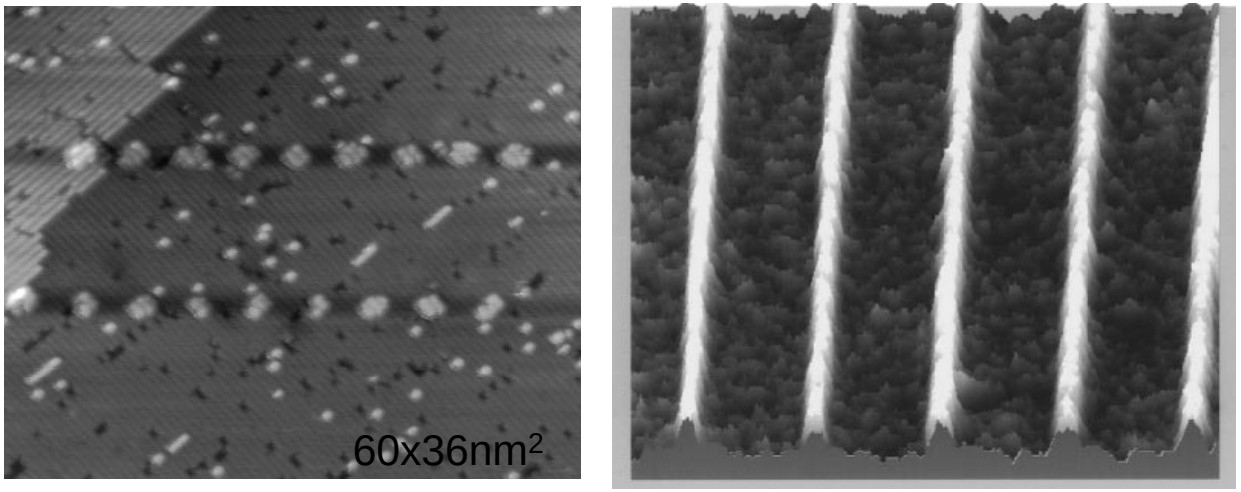

Images of oxide features patterned with SPM tip on Si(111)

D. Stievenard et al, *Prog. Surf. Sci.* 81, (2006); R. M. Feenstra *Nanotech.*, **18** 044015 (7pp) (2007)
J.A. Dagata et al, *APL* 56, 2001 Ph. Avouris et al., *APL* 72, 1997; O. Bikondoa et al, Nat. Mater. **5,** 189 (2006)

Bias-induced oxidation

The drop in I_{tunnel} caused by a space charge build up within the oxide overlayer due to the large number of charged defects, inhibiting further growth.

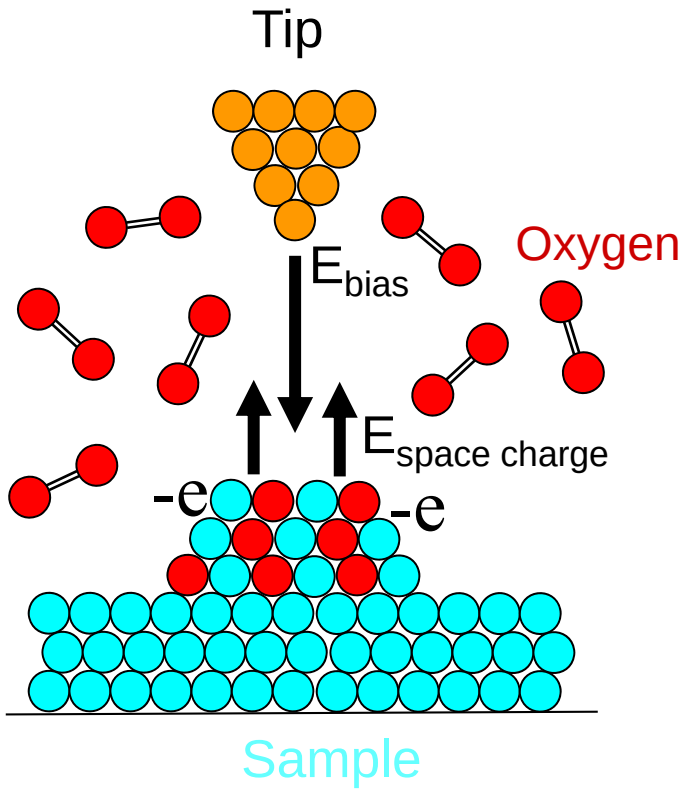

D. Stievenard et al, Applied Physics Letters 70 (1997) 3272

Possible mechanisms for bias-induced oxidation

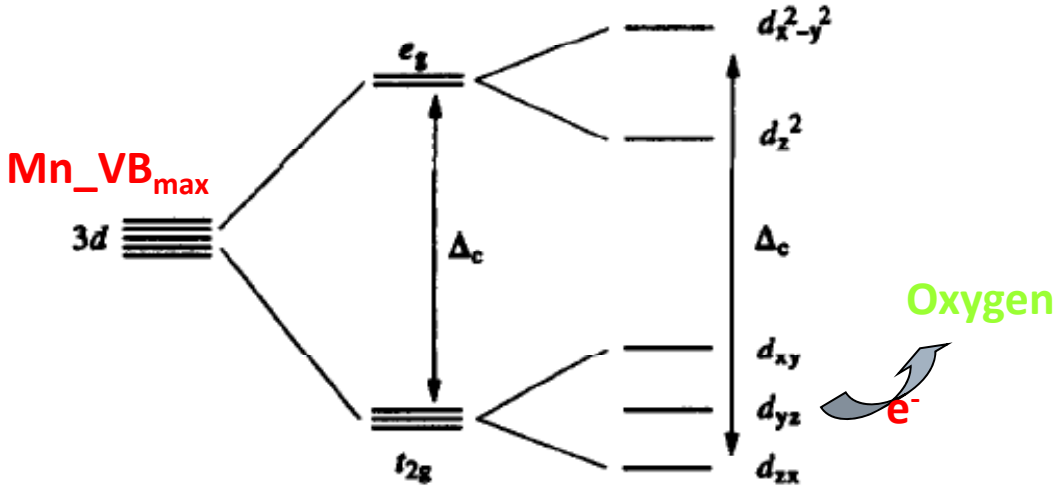

A. Chikamatsu et al, Phys. Rev. B **73**, 195105 (2006)
H. Kamata et al, J. Phys. Chem. Solids **56**, 943 (1995)

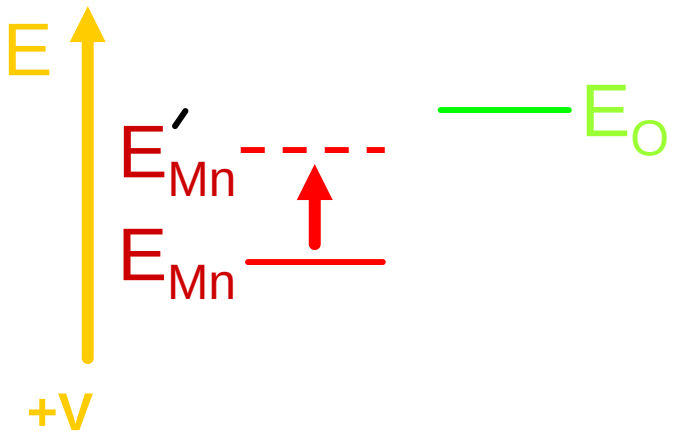

Ph. Avouris, *Surface Science* 363, 1996

- At +V → upward bending of the electronic bands and shifts Mn/La/Sr electronic states to higher energy.
- Reduce or null the activation barrier for oxygen chemisorption and binding → bonding tuned by STM, localized at the tip – LSM surface at high temperature.
- V_{th} temperature dependence? → related to temperature dependence of the chemical potential?

Key observations and hypothesis

- Could STM-induced excitations allow to probe the surface-oxygen bonding activation barrier?
  - T-, t-, and V-dependent drop in I_{tunnel} → chemical reaction.

Hypothesis: $V_{th,}$ at a given temperature, could be used as probe of electrochemical polarization for surface-oxygen bonding, with both chemical and electric potential energy contributions.

Key observations and hypothesis

- What is the effect of thickness of dense thin-film $La_{0.7}Sr_{0.3}MnO_3$ (LSM) cathodes on surface, composition, and electronic structure?
  - Thinner LSM surfaces →
    - have A-site rich surfaces in AES,
    - are more resistive (large E_G) in STS (RT),
    - show surface limited ORR in EIS.

→Thin LSM cathode surfaces:

Film thickness ←→ elastic strain

Effect of strain?
Surface composition, electronic exchange, and anion transport

Effect of strain:
Surface composition, surface chemisorption

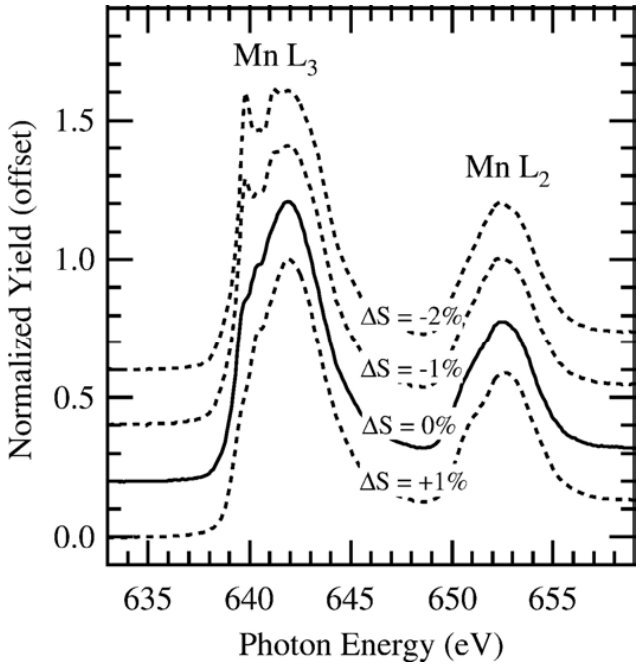

Mn $L_{2,3}$ edge XAS spectra for $La_{2/3}Ca_{1/3}MnO_3$ thin films as a function of substrate induced stress in the films.

Lussier et al. *Thin Film Solids*, **516**, 2008

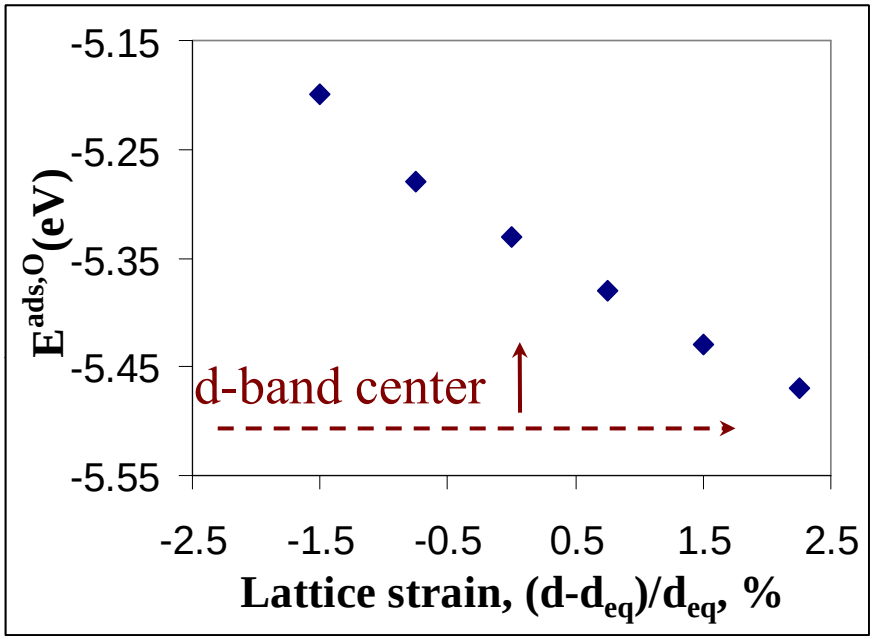

Effect of lattice strain, $(d-d_{eq})/d_{eq}$, on a Ru(0001) surface on the binding energy of atomic oxygen

(Figure adopted from Mavrikakis et al. *PRL* **81**, 1998)

Key observations and hypothesis on LSM surface

- Thickness and deposition conditions influence the initial surface composition:
  - Thinner film and high T_{dep} → higher A/B
- Electronic behavior varies strongly:
  - Multiple co-existing phases, defects, strain.
- Tunneling conductance increase and decrease with temperature:
  - Structural transformation at lower temperature, and A/B increase at higher temperature.
- T-, t-, and V-dependent drop in I_{tunnel} → chemical reaction.
  - $V_{th,}$ at a given temperature, could be used as probe of electrochemical polarization for surface-oxygen bonding.
- *Ex situ* electrochemical surface chemistry is not conclusive, yet.
  - Increase in A/B ratio common between STS results here and electrochemical results from literature on LSM and LSCF.

Future directions

- Follow on each hypothesis discussed
  - Currently: origin of local tunneling differences
    - Microscopy with chemical analysis
  - Systematic electrochemical and STS/AES comparisons

- Extend to $La_{0.6}Sr_{0.4}Co_{0.2}Fe_{0.8}O_3$

- Compare / contrast:
  - *In situ – ex situ* surface structures and compositions and electrochemistry from the ANL groups.
  - STS data with the soft x-ray and electron spectroscopy from UNLV group and with theory – Stanford – group.

New samples & experimental conditions

(Difference → YSZ substrates annealed at 1450°C prior to deposition)

10nm-(x3), 50nm-(x2)-, 100nm-(x3), 200nm-(x2) for STM+AES

10nm-(x2), 50nm-(x1), 100nm-(x1) for Electrochem.+AES

(T_{dep} = 700°C and 800°C. 800°C made smoother 100nm-thick LSM)

STM samples

(presented here: one for each thickness)

AES as received from CMU (as received)

↓

Clean carbon from surface at 450-500°C in ~10^{-7}mbar O_2

↓

AES after surface cleaning (after oxygen cleaning)

↓

STM/STS at RT→580°C→RT in 10^{-4}-10^{-3}mbar O_2 (STM treatment)

↓

AES after STM treatment (after STM treatment)

↓

AES at RT→580°C→RT in 10^{-6}mbar O_2 (AES treatment)

Electrochem. samples

(presented here: 10- and 100nm-thick samples)

AES as received from CMU (as received)

↓

Ex situ electrochemical treatment at 600-700°C
0.3V for 1hour (Potentiostatic)
0.3A for 1hour (Galvanostatic)

↓

AES after electrochemical treatment (after p-static, or g-static)

Summary of previous results

	10-50 nm thick LSM cathode	100 nm thick LSM cathode
STM/STS Surface e^- - exchange	- $R_{tun,thin}$ >> - Large Eg - No correlation with boundaries	- $R_{tun,thick}$ - Small → Large Eg, and metallic regions - e^- exchange greater at some boundaries
EIS O_2-reduction	Surface exchange-limited	Bulk diffusion, and YSZ interface
AES (La+Sr)/Mn	4.7-3.5 >> ⇑	2.5 ⇑
Heat-treatment in reducing conditions	(La+Sr)/Mn ⇑ $R_{tunneling}$ ⇑, Large Eg	(La+Sr)/Mn ⇑ $R_{tunneling}$ ⇑, Large Eg

44

Surface topography of dense thin-film (110) $La_{0.7}Sr_{0.3}MnO_3$ (LSM) on (111) 8% Y_2O_3-ZrO_2 (YSZ)

10nm-thick LSM
Z-range: 7 nm

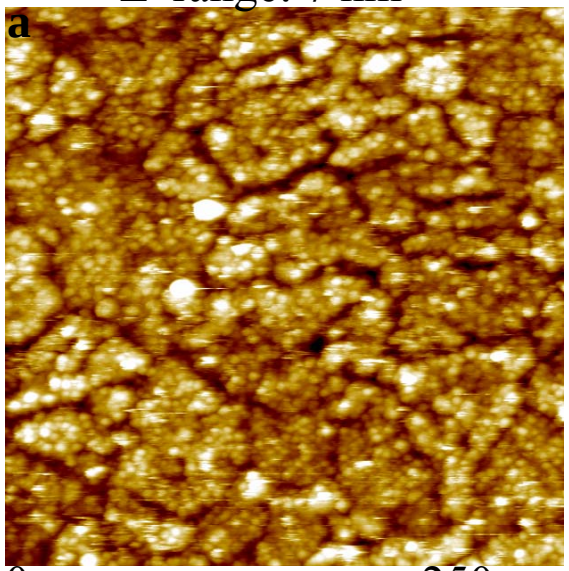

0 nm 250 nm

100nm-thick LSM
Z-range: 20 nm

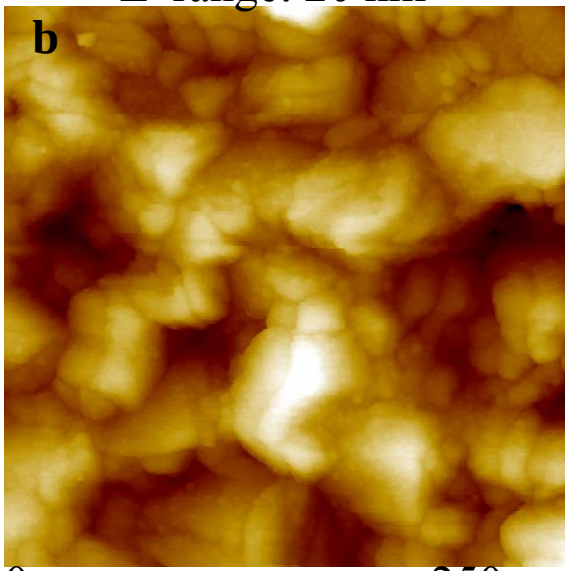

0 nm 250 nm

100nm-thick LSM
Z-range: 23 nm

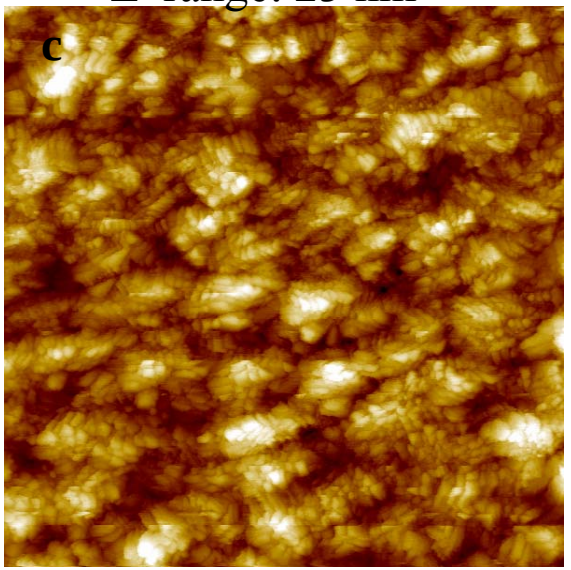

0 nm 1000 nm

(a) 20-50nm size grains, 2-5nm and islands of atoms on the as-deposited 10nm-thick LSM, (b-c) clusters of 10's to 100's nm size on the as deposited 100nm-thick LSM, both on YSZ.

→ Is the non-uniform structure of electrode surfaces associated with non-uniform electrochemical activity?

45

50nm-thick LSM surface topography

RT, $P_{O2\text{-}surface} = 10^{-10}$mbar

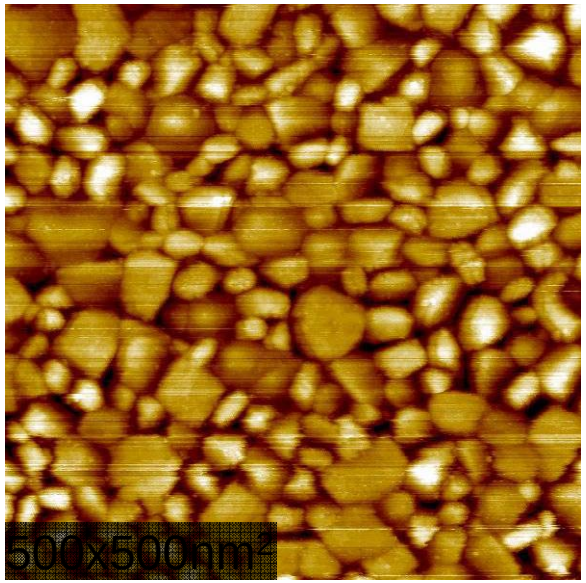

- Various sizes of clusters co-exist. No large islands.
- Step-edges resolved both at RT and at 580°C in oxygen.

580°C, $P_{O2\text{-}surface} = 10^{-4}$-$10^{-3}$ mbar

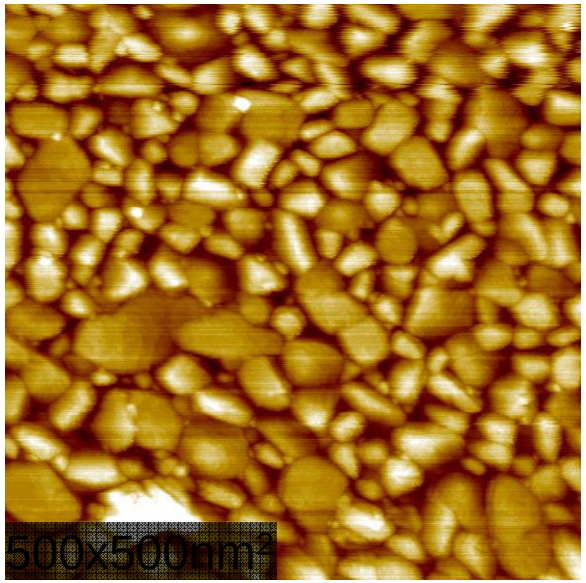

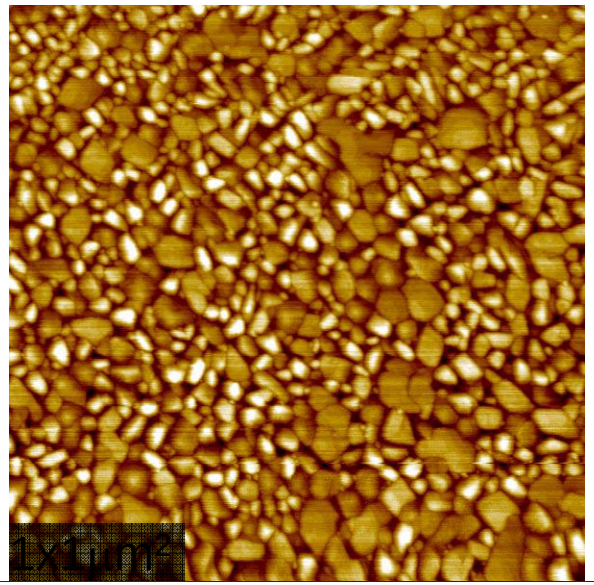

No grain growth within ~12 hrs) at high temperature, probed *in situ*.

100nm-thick LSM surface topography

RT, $P_{O2\text{-}surface} = 10^{-10}$mbar

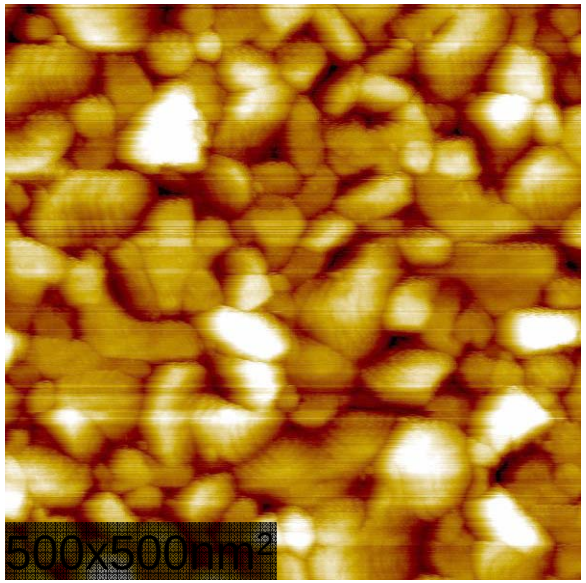

580°C, $P_{O2\text{-}surface} = 10^{-4}$-$10^{-3}$ mbar

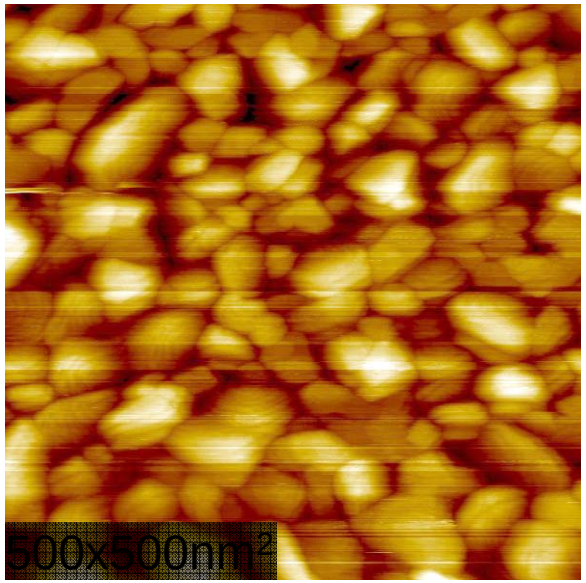

- Various sizes of clusters co-exist. No large islands.
- Step-edges resolved both at RT and at 580°C in oxygen.

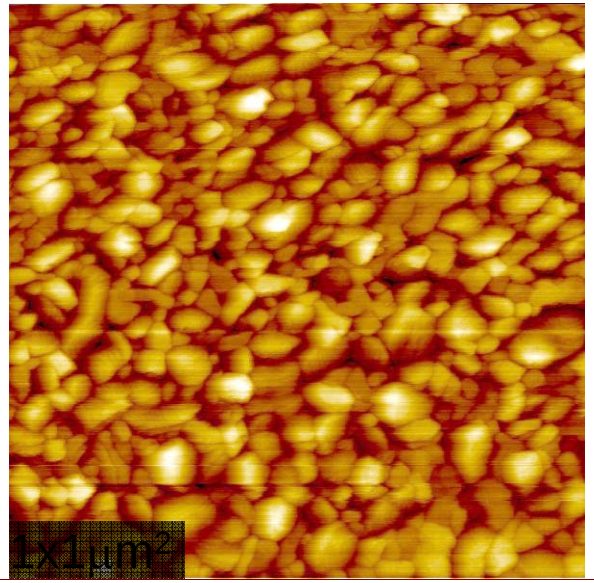

No grain growth within ~12 hrs) at high temperature, probed *in situ*.

Variation in the electronic behavior probed by STS

10nm-thick

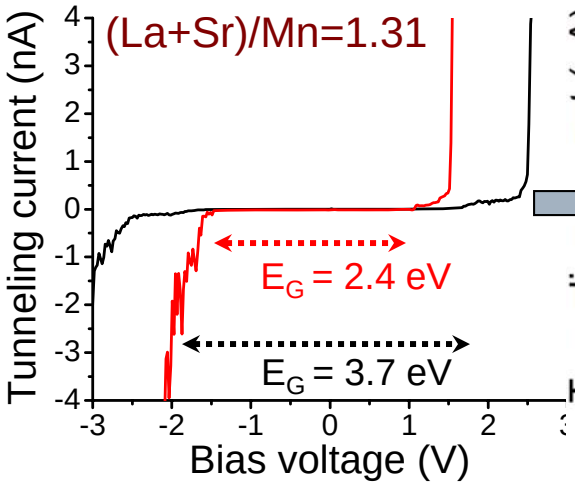

50nm-thick

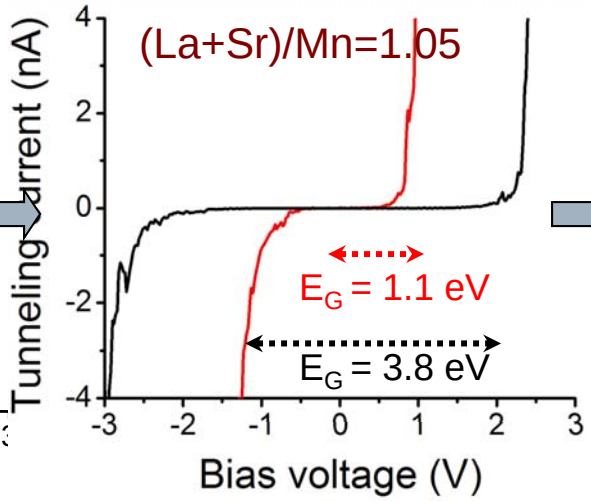

100nm-thick, T_{dep} = 700°C

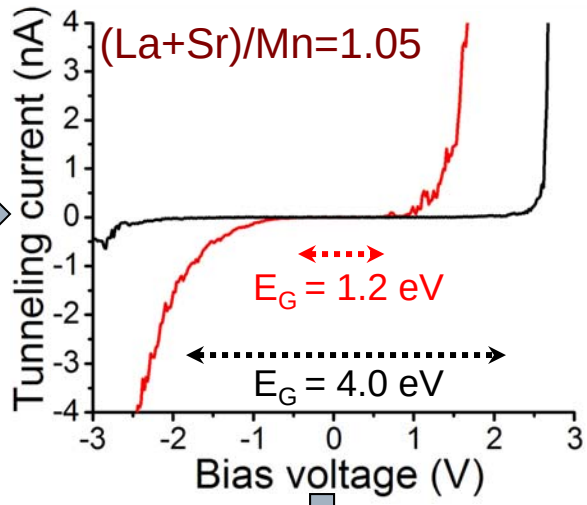

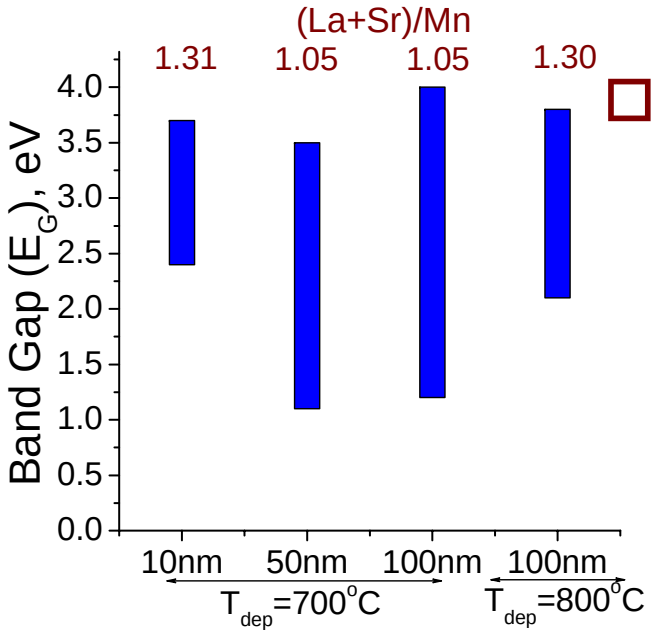

- "Larger thickness" and "higher T_{dep}" lead to:
  - larger A/B,
  - more insulating STS.

100nm-thick, T_{dep} = 800°C

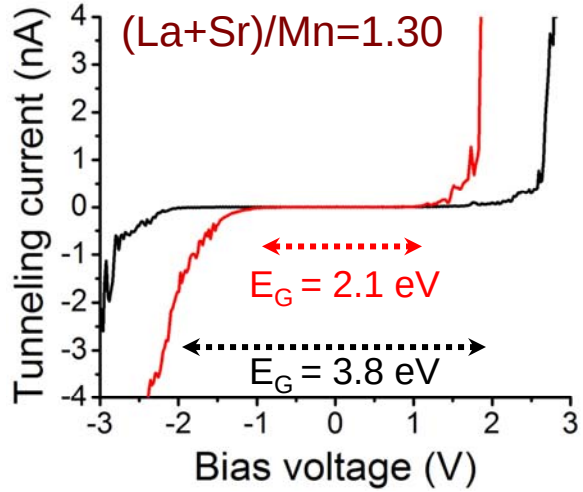

I_{tunnel} correlated with boundaries and/or domains and/or strain:

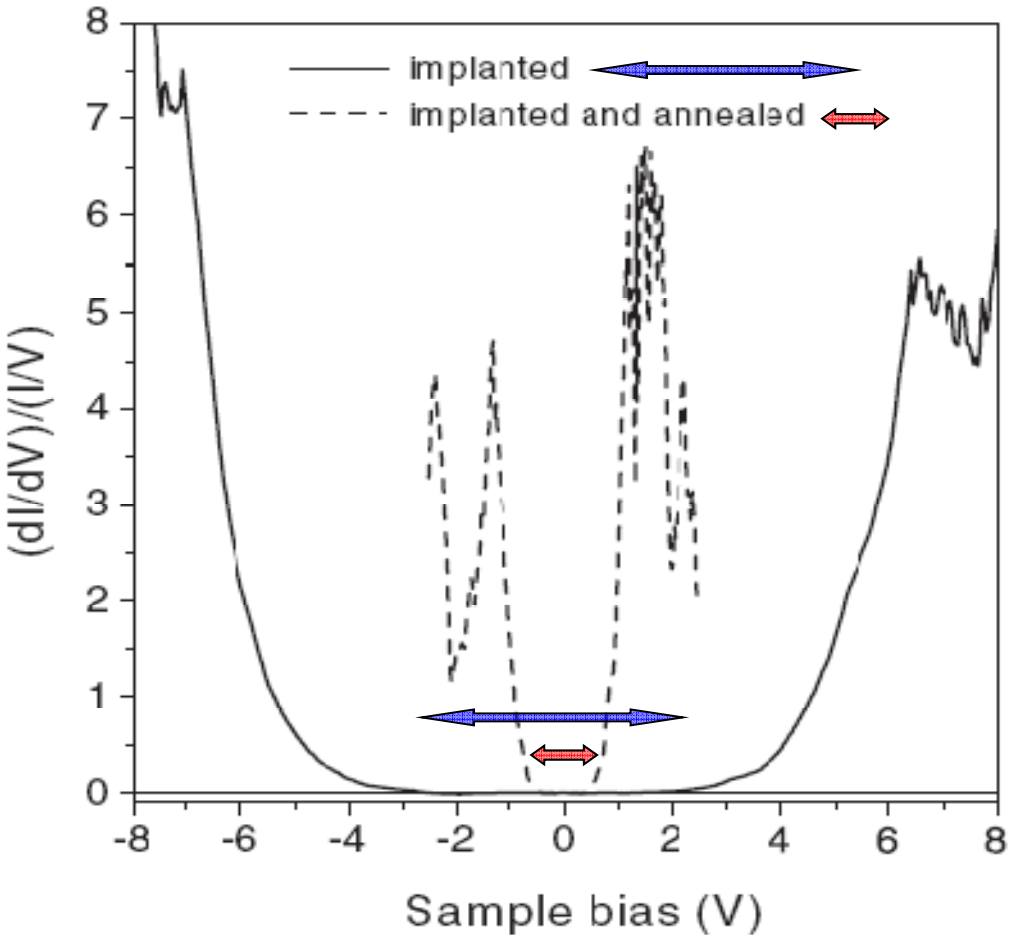

E Nogales et al. *Semi. Sci. Tech.*, **16** (2001).

B-doped Si nano-crystallites:- as-implanted, and annealed

Reduction in band gap attributed to the grain size increase and strain relaxation in the annealed film.

49

Variation of STS Spectra: possible reasons
1) Multiple phases on the surface

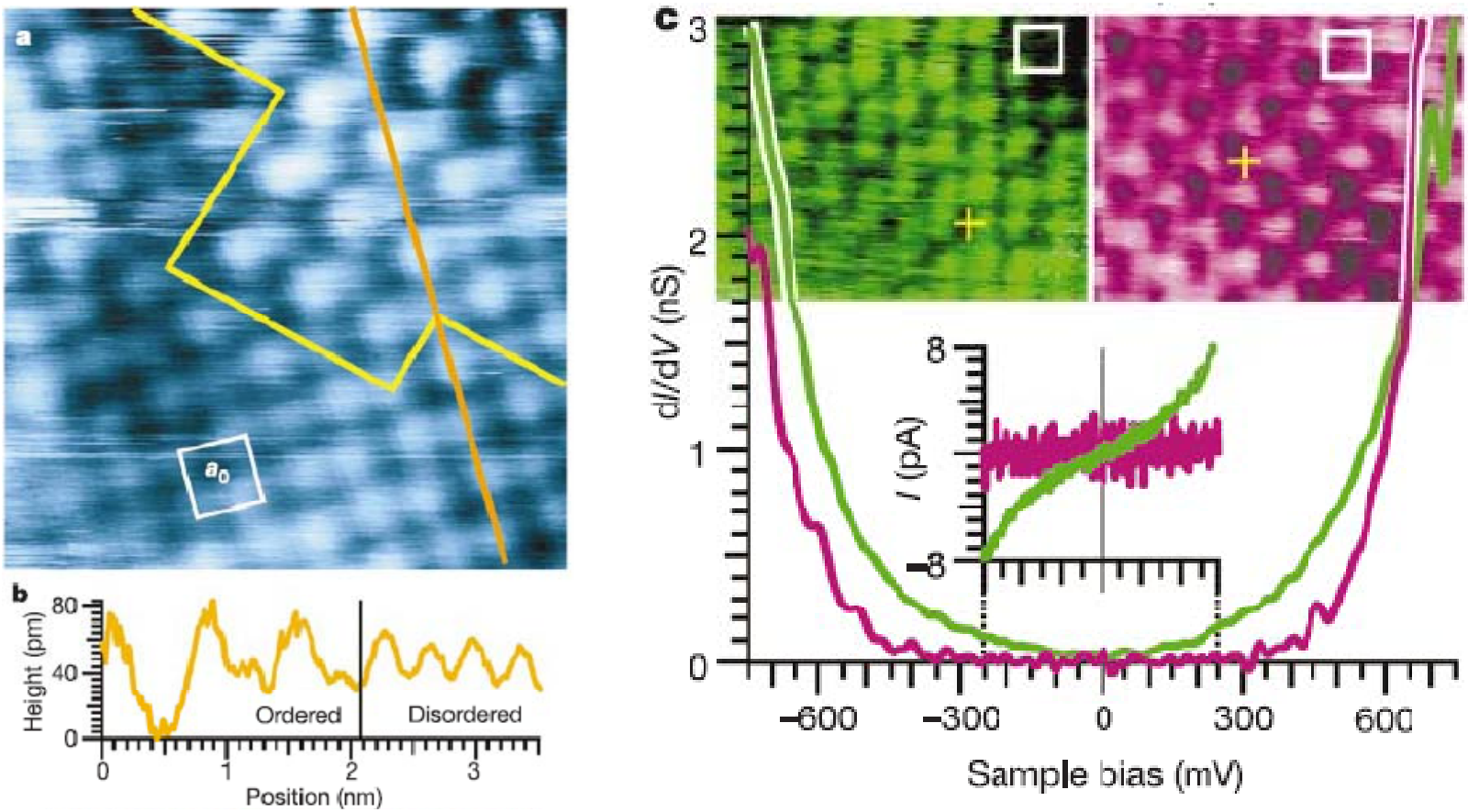

Ch. Renner et al, *Nature*, 416 518 (2002)

Topographic and spectroscopic atomic-scale study of $Bi_{0.24}Ca_{0.76}MnO_3$, show the phase separation into metallic and insulating surface regions.

I_{tunnel} correlated with grain boundaries: Chemical or structural reasons?

- Defect chemistry variation on the surface and in the vicinity of GB due to cation segregation?

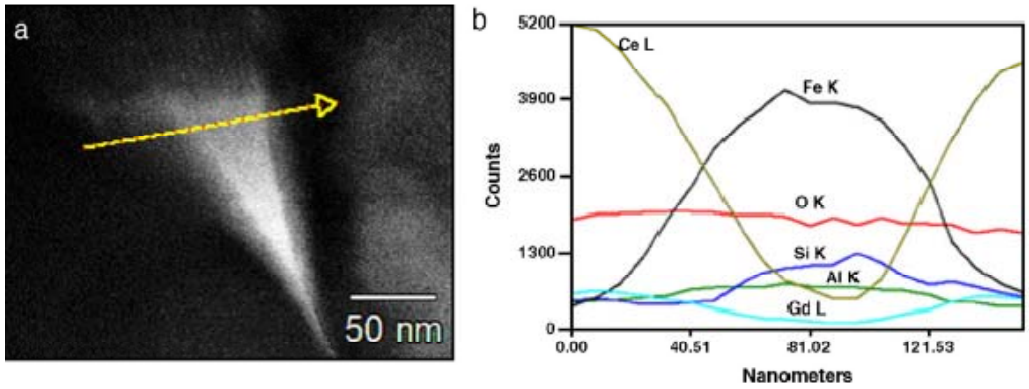

Segregation of Fe to triple-junctions

→ defect chemistry with greater oxygen vacancy concentration.

→ higher ionic conductivity in nanocrystalline doped ceria.

H. Parades, S. Kim, *SSI* **177** (2006)

- Structural disorder at GB, leading to a net charged core with surrounding space charge region.

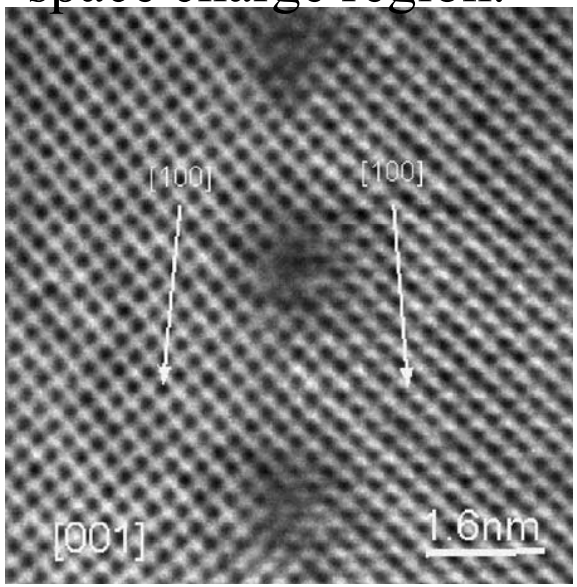

Dislocation cores at low angle tilt GB in STO:

→ Positive charge at GB due to oxygen depletion, surrounded by space charge.

Zhang et al. *Acta Mater*. **53** (2005)

- 200nm LSM, annealed at 1atm at 800^{o}C for 1 hour.

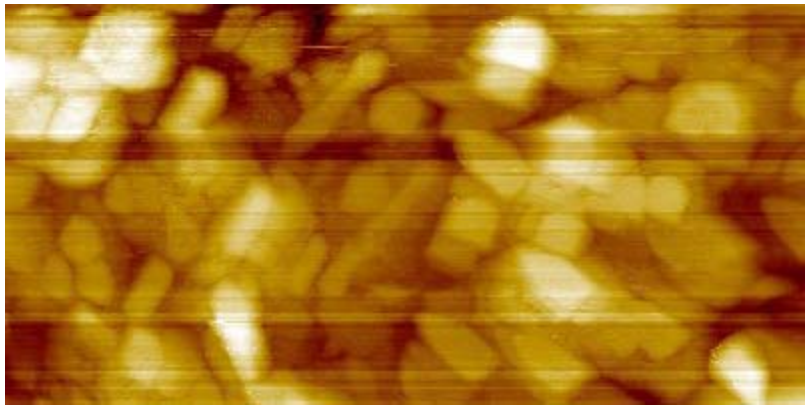

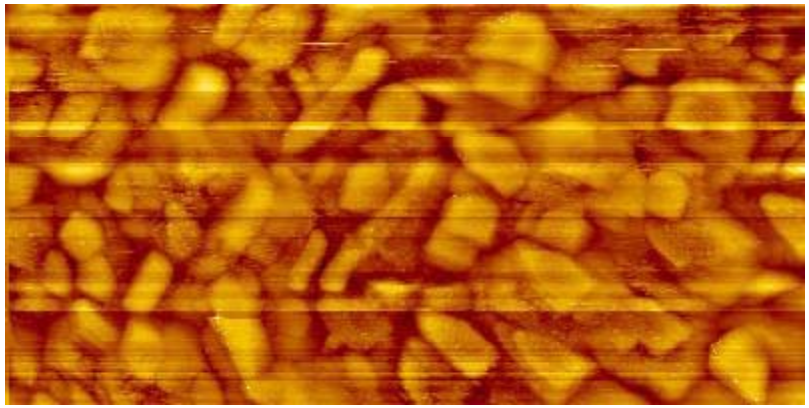

Possible mechanisms for bias-induced oxidation

Ab initio studies indicate that the favorable site for oxygen binding on LSM surface is on Mn-cations.

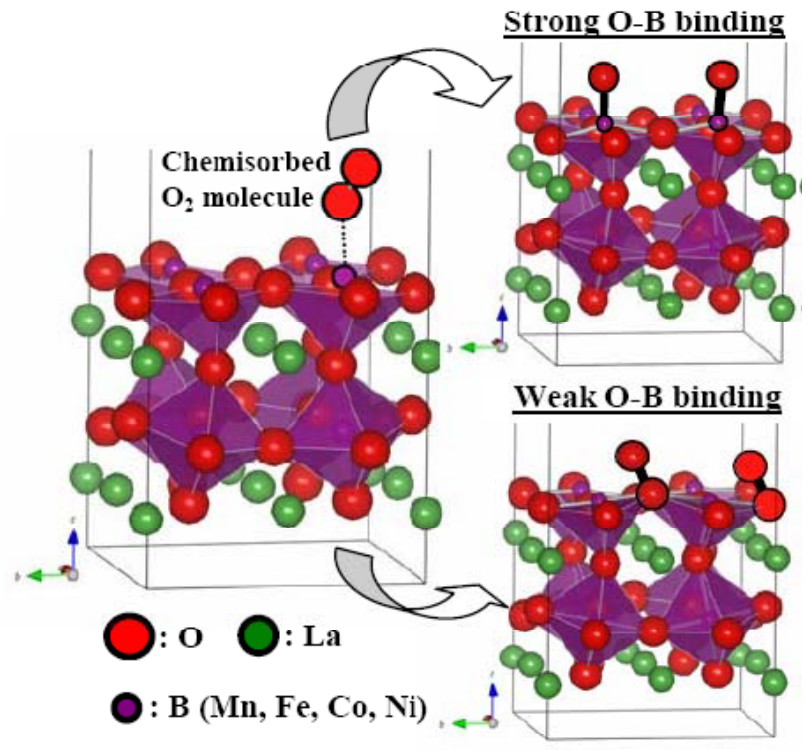

Figure 2: Two possible O_2 dissociation final states depending on the O-B binding strength.

Y-L. Lee, D. Morgan, et al., 214th Meeting Electrochemical Society, Honolulu, HI, 2008

- Multiple binding sites are possible.
  - E.g. Atop and bridge sites for B-O binding on La(Mn, Fe,Co)O_3

- $E_{adsorption}$ for O on Mn on the defective:
  - $LaMnO_3$: 1.82 eV
  - $(La,Sr)MnO_3$: 1.93 - 2.79 eV
- $E_{adsorption}$ for O on MnO_2 terminated surface: 2.2 eV

M. Choi, Chemistry of Materials 19 (2007) 1690
M. Choi et al, Angewandte Chemie Int. Ed., 46, (2007) 7214

Example: Nanometer-scale phase separation in $Pr_{0.68}Pb_{0.32}MnO_3$

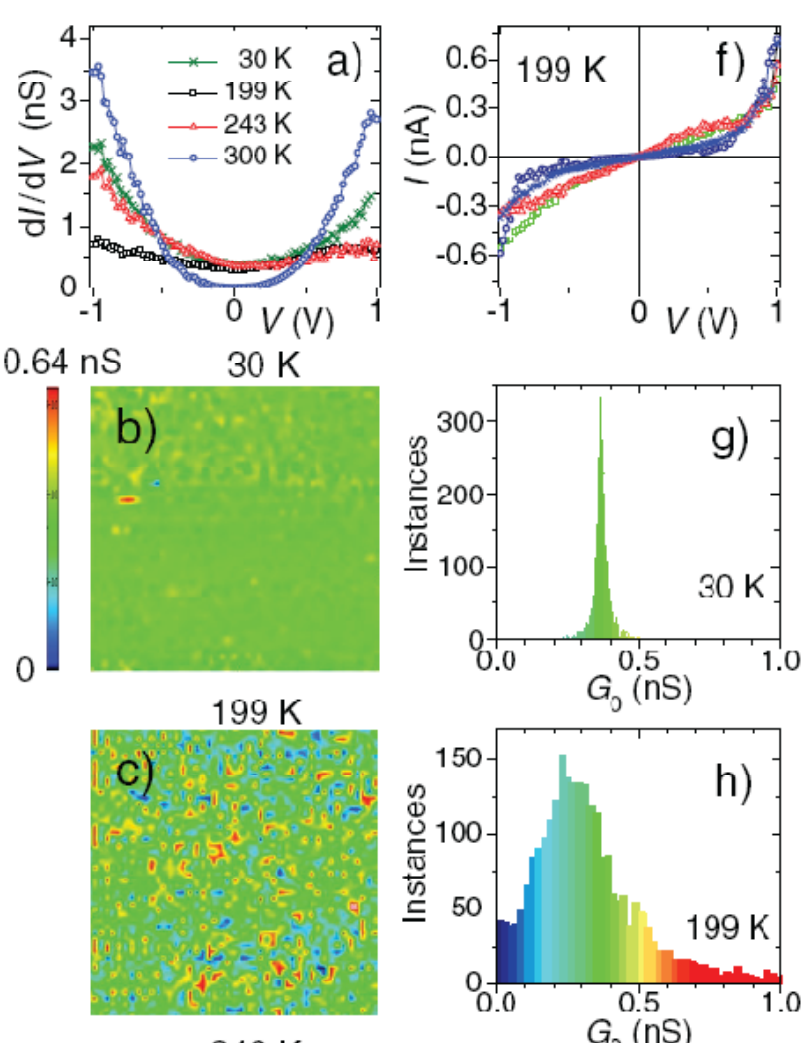

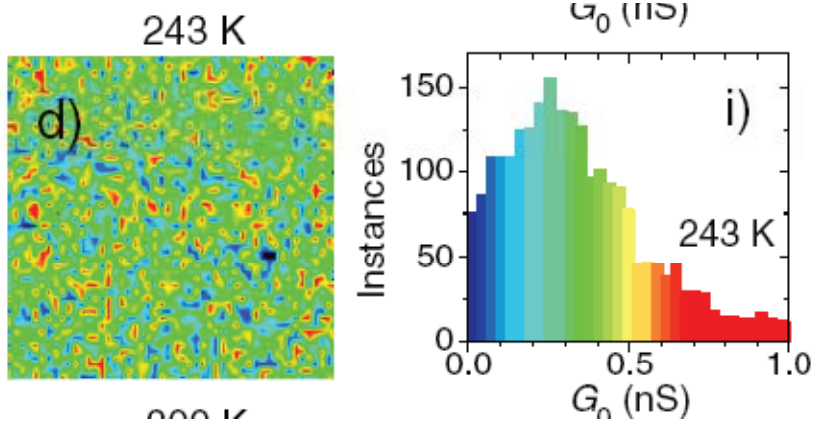

Fig. 3: (a) G-V curves averaged over $50 \times 50\,\mathrm{nm}^2$ at 30, 199, 243 and 300 K indicating metallic ($T < T_{MI} \approx 255\,\mathrm{K}$) and insulating behavior. (b)–(e) Maps ($50 \times 50\,\mathrm{nm}^2$) of the local zero-bias conductance G_0 for the same temperatures, *i.e.* through T_C and T_{MI}. The color encodes the value of G_0, see (b). (f) I-V curves at $T = 199\,\mathrm{K}$ obtained at four different positions to illustrate the spatially inhomogeneous conductance, as shown for G_0 in (c). The curves are color-coded according to their G_0 value. (g)–(j) Histograms of G_0 for the maps (b)–(e) using the same color code. Inset to (j): zoom into low G_0.

S. Rossler et al., *EPL*, **83,** 2008

54

Electronic properties evolve on the surface at high temperature and oxygen dosing at reducing conditions

- Large variation in the $E_{g.}$
- High tunneling conductance.

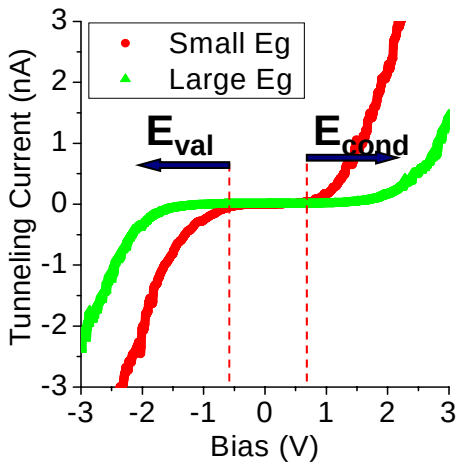

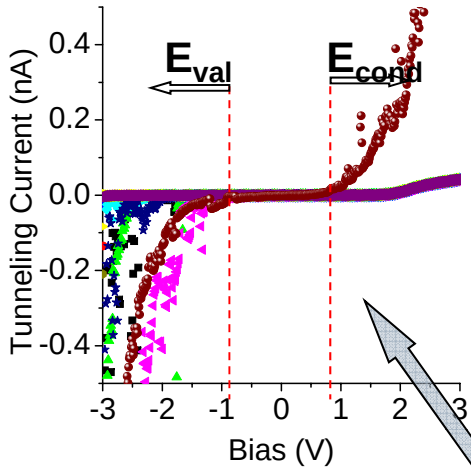

- Larger E_g compared to as prepared LSM.
- Lower tunneling conductance, insulating.

Now have another view of these…

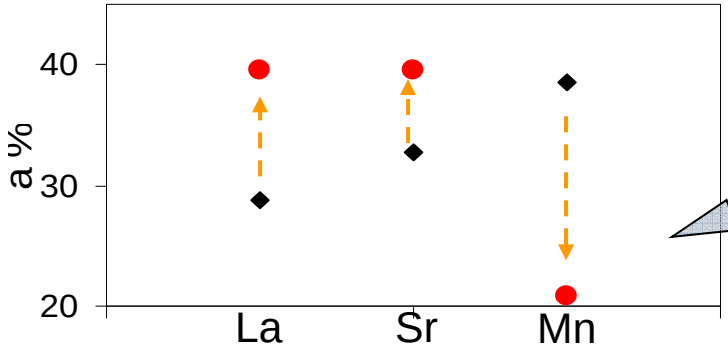

Heat treatment under reducing conditions → insulating in surface electron exchange (STS) + enriched in La+Sr (AES)

"Strong oxygen binding and high O-vacancy formation energies suggest LaO-terminated surfaces are catalytically inactive" Y-L. Lee, D. Morgan, et al., 214th Meeting Electrochemical Society, Honolulu, HI, 2008

55

Surface composition and surface exchange activity upon reducing PO_2 and polarization treatment

Before and after heat treatment at 550°C and reducing PO_2

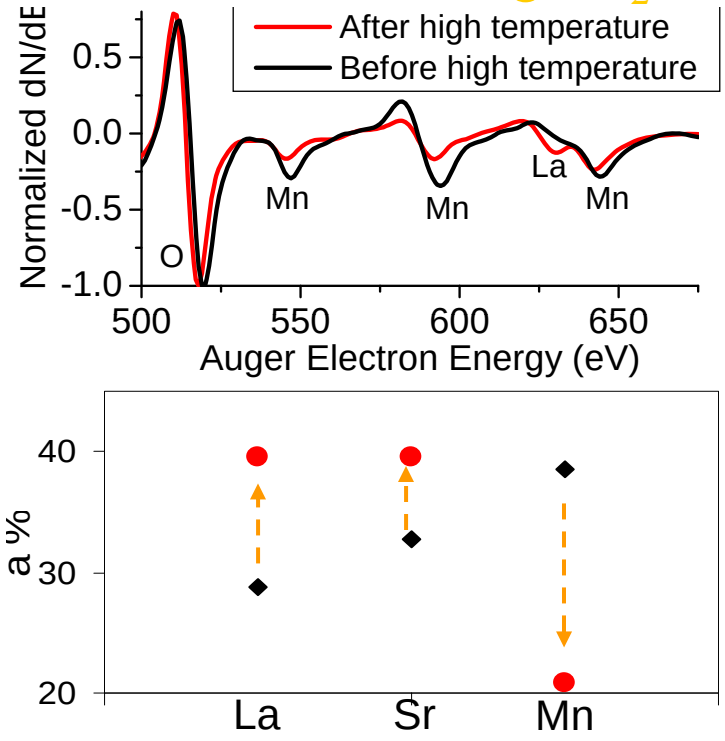

Before and after electrochemical treatment at 660°C and reducing η

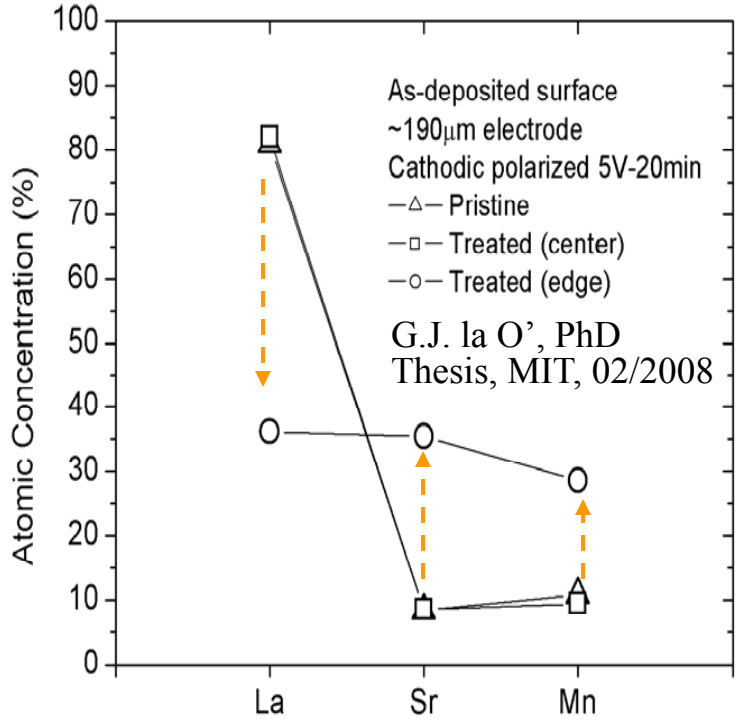

Common: Decrease in La → enhance electronic or electrochemical property

Contrast: Increase in La in reducing (cathodic-like) PO_2, **vs**.
decrease in La in cathodic potential.

→ Electronic or ionic current, in addition to surface potential, can alter the surface compositions.

56

Temperature dependence of electronic behavior

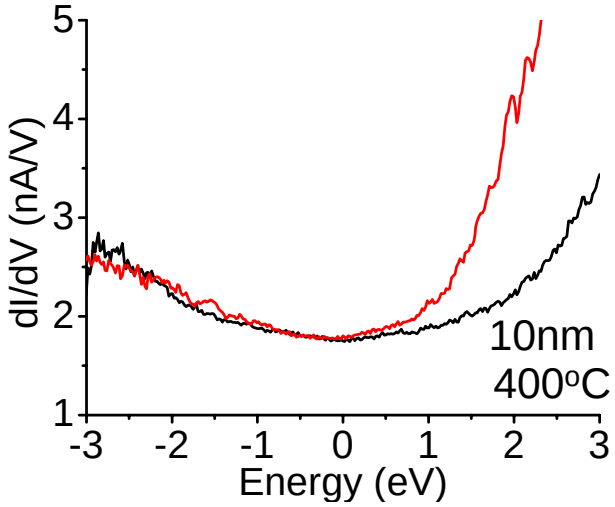

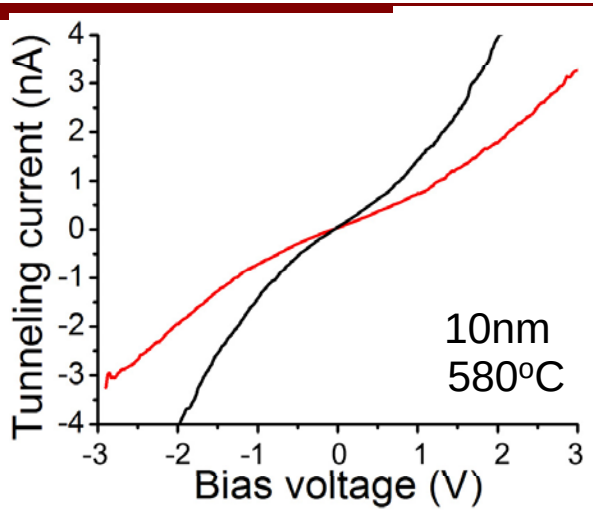

- Electronic behavior at high temperature, metallic nature with a large range in electron tunneling conductance.

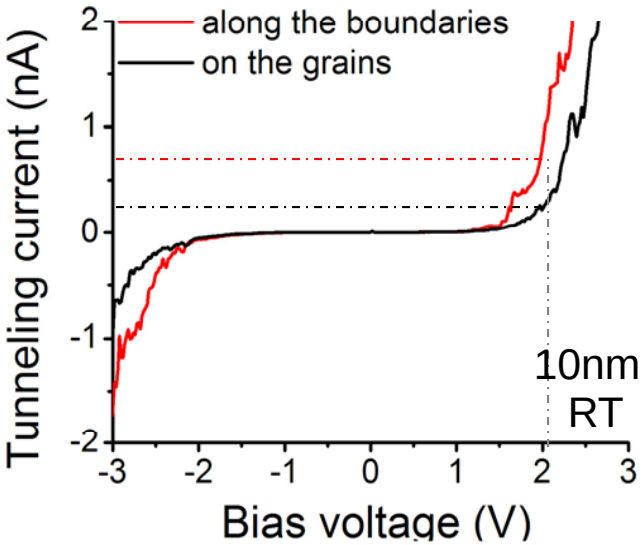

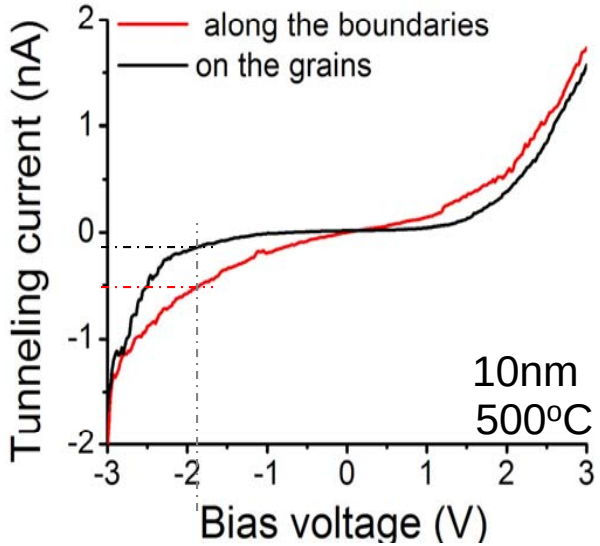

- Boundary and bulk tunneling conductance differ both at RT and at high temperatures.

High temperature chemical and electronic behavior

- The band gap → metallic transition: A structural transformation at the surface, e.g. from an orthorhombic phase (characterized by a strong Jahn–Teller distortion) as an insulating paramagnetic state, to a rhombohedral phase with a ferromagnetic metallic state.

TABLE I. Conditions for the crystal growth by the FZ method and results of the characterization of $La_{1-x}Sr_xMnO_3$. $\%Mn^{4+}$ shows the nominal Mn valence of the obtained crystal (ideally x for the stoichiometric sample) obtained by the redox titration. EPMA indicated that the metal composition (La/Sr/Mn) is nearly identical with the prescribed one within the experimental accuracy of ±2%. T_N, T_C, and M_s mean the Néel temperature, the Curie temperature, and the saturated magnetization, respectively.

x	Method	Atmosphere	$\%Mn^{4+}$	T_N (K)	T_C (K)	Structure	M_s (μ_B/Mn site)
0.00	FZ	Ar	2	143		Orthorhombic	
0.05	FZ	Ar	7	139		Orthorhombic	
0.10	FZ	air	12		145	Orthorhombic	3.6
0.15	FZ	air	15		238	Orthorhombic	4.2
0.175	FZ	air	17		283	Rhombohedral	4.0
0.20	FZ	air	19		309	Rhombohedral	3.9
0.25	FZ	air	19		342	Rhombohedral	3.9
0.30	FZ	Ar 50% O_2 50%	28		369	Rhombohedral	3.5
0.40	FZ	Ar 50% O_2 50%	36		371	Rhombohedral	3.4
0.60	FZ	O_2	54		357	Rhombohedral	3.3

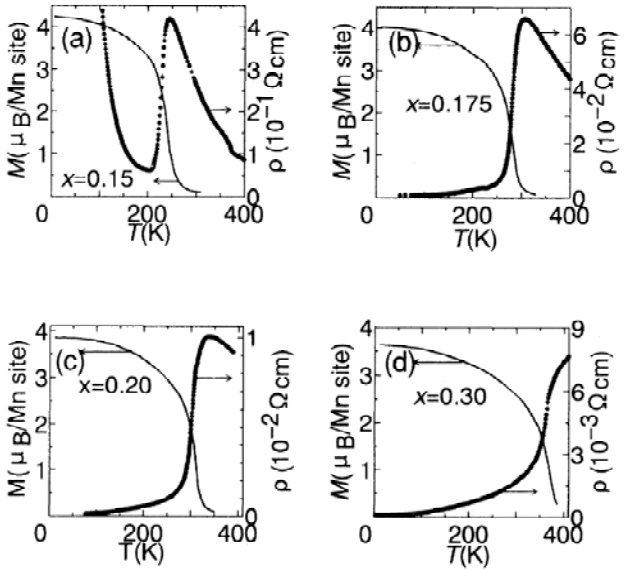

FIG. 3. Correlation between the temperature dependence of resistivity and magnetic moment for $La_{1-x}Sr_xMnO_3$ crystals; (a) x=0.15, (b) x=0.175, (c) x=0.20, and (d) x=0.30. All the data shown were taken with a magnetic field of 0.5 T.

A. Urushibara et al, Physical Review. B (51) 1995 14103

Effect of electrochemical treatment

Impedance (10nm- and 100nm-thick)

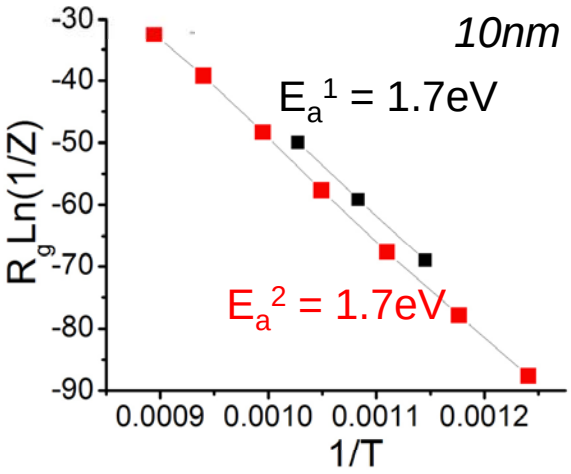

E_a=1.7eV: surface limited,
E_a=2.5eV: bulk diffusion in oxygen-reduction

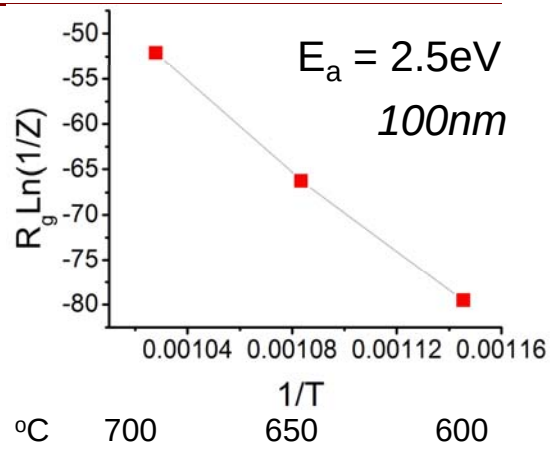

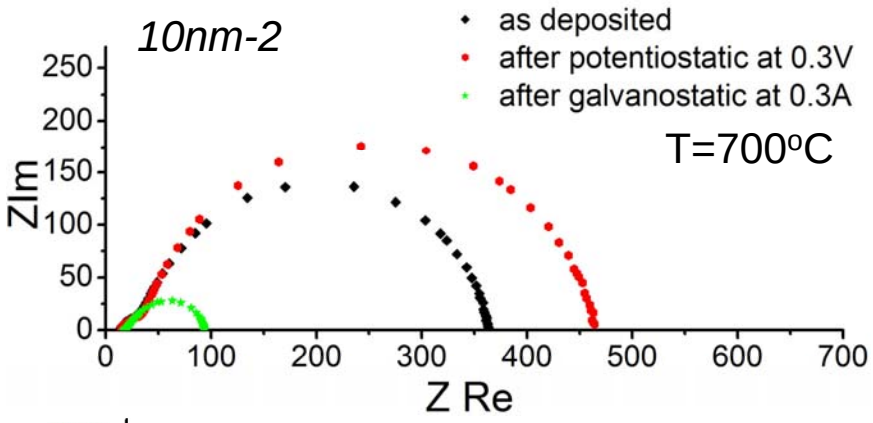

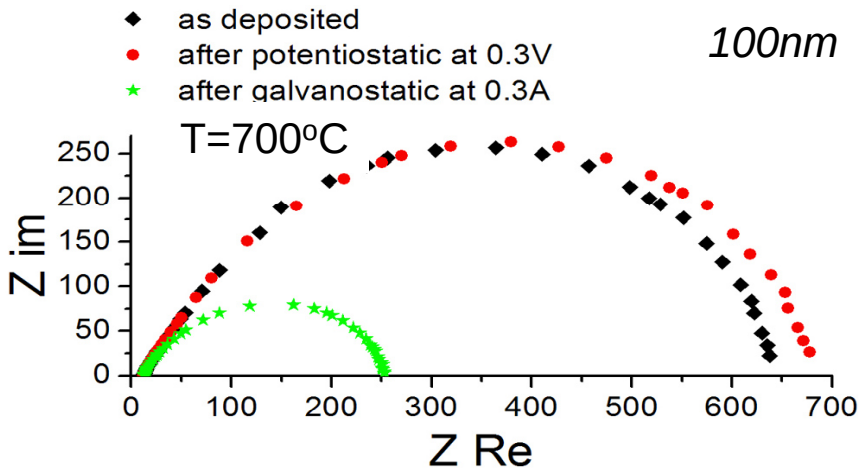

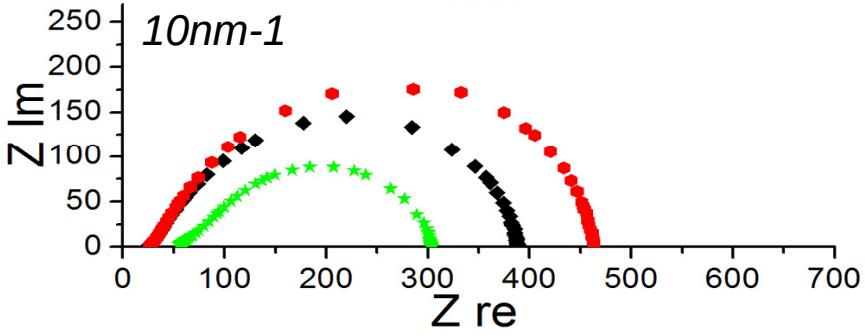

Degrade upon pontentiostatic, and improve upon galvanostatic treatment.

J. Van Herle et al., *Electrochim. Acta*, 41 (1996)
M. J. Jorgensen et al., *J. Electrochem. Soc.* 148 (2001)
Y. Arachi et al., *Solid State Ionics*, 121 (1999)
G.J. la O' et al., *J. Electrochem. Soc.*, 154(4) (2007)